Phylogenetic relationships and systematics of the Amazonian poison frog genus *Ameerega* using ultraconserved genomic elements

Wilson X. Guillory[1,*], Connor M. French[1,2], Evan M. Twomey[3], Germán Chávez[4], Ivan Prates[5], Rudolf von May[6], Ignacio De la Riva[7], Stefan Lötters[8], Steffen Reichle[9], Shirley J. Serrano-Rojas[10,11], Andrew Whitworth[11], and Jason L. Brown[1]

[1]Southern Illinois University, Carbondale, IL, USA. [2]Department of Biology, Graduate Center, City University of New York, 365 5th Ave, New York, NY, 10016, USA. [3]Pontificia Universidade Católica do Rio Grande do Sul (PUCRS), Porto Alegre, Brazil. [4]División de Herpetología - CORBIDI, Lima, Peru. [5]Smithsonian Institution, National Museum of Natural History, Division of Amphibians and Reptiles, 10th and Constitution Ave, NW, Washington, DC, 20560-0162, USA. [6]Biology Program, California State University Channel Islands, 1 University Drive, Camarillo, CA, 93012, USA. [7]Museo Nacional de Ciencias Naturales -CSIC, Madrid, Spain. [8]Universität Trier, Trier, Germany. [9]Museo de Charupas, Santiago de Chiquitos, Bolivia [10]Universidad Nacional de San Antonio Abad del Cusco, Cusco, Peru. [11]Institute of Biodiversity, Animal Health and Comparative Medicine, College of Medical, Veterinary and Life Sciences, University of Glasgow, Glasgow, United Kingdom.
[*]corresponding author, email: wilsonxguillory@gmail.com, tel: +1-478-244-7461

Abstract

The Amazonian poison frog genus *Ameerega* is one of the largest yet most understudied of the brightly colored genera in the anuran family Dendrobatidae, with 30 described species ranging throughout tropical South America. Phylogenetic analyses of *Ameerega* are highly discordant, lacking consistency due to variation in data types and methods, and often with limited coverage of species diversity in the genus. Here, we present a comprehensive phylogenomic reconstruction of *Ameerega*, utilizing state-of-the-art sequence capture techniques and phylogenetic methods. We sequenced thousands of ultraconserved elements from over 100 tissue samples, representing almost every described *Ameerega* species, as well as undescribed cryptic diversity. We generated topologies using maximum likelihood and coalescent methods and compared the use of maximum likelihood and Bayesian methods for estimating divergence times. Our phylogenetic inference diverged strongly from those of previous studies, and we recommend steps to bring *Ameerega* taxonomy in line with the new phylogeny. We place several species in a phylogeny for the first time, as well as provide evidence for six potential candidate species. We estimate that *Ameerega* experienced a rapid radiation approximately 7-11 million years ago and that the ancestor of all *Ameerega* was likely an aposematic, montane species. This study underscores the utility of phylogenomic data in

improving our understanding of the phylogeny of understudied clades and making novel inferences about their evolution.

Keywords: phylogenomics, UCEs, *Ameerega,* systematics, Dendrobatidae, amphibians

1. Introduction

Neotropical poison frogs (Dendrobatidae) are a charismatic and well-studied anuran clade, but evolutionary relationships among dendrobatids remain controversial, especially for certain genera. Poison frogs are important study systems in pharmacology and toxicology (Daly et al., 1985; Tarvin et al., 2017, 2016), behavior (Brown et al., 2008; Wells, 1980), sexual selection (Limerick, 1980; Summers et al., 1999), color evolution (Maan and Cummings, 2009; Wang and Shaffer, 2008), speciation (Twomey et al., 2016, 2014), and biogeography (Brown and Twomey, 2009; Noonan and Gaucher, 2006). Understanding their phylogenetic relationships is instrumental to improving the group's systematics and providing an evolutionary framework for investigations in these fields, and also for supporting the identification of appropriate study systems.

The poison frog genus *Ameerega* Bauer, 1986 is an example of an understudied taxon whose systematics are poorly resolved. Consisting of 30 described species (Table 1) in the subfamily Colostethinae (Grant et al., 2017; Guillory et al., 2019), most *Ameerega* are found in restricted ranges along the eastern versant of the central and northern Andes from Colombia south to Bolivia, reaching their highest diversity in the eastern Andean foothills of central Peru. However, several taxa, such as *A. trivittata* and *A. hahneli,* are widespread throughout the Amazon Basin, and one clade (the *braccata* group) inhabits the dry savannahs from eastern Brazil to Bolivia. In coloration, *Ameerega* range from cryptic to highly conspicuous – although their toxicity is not well-studied (though see Darst et al., 2006; Mebs et al., 2010; Santos et al., 2016), it is assumed that the presence of toxic alkaloids in their skin corresponds to their degree of aposematism, as with other dendrobatids (Summers and Clough, 2001). As *Ameerega* is one of the most speciose dendrobatid genera, and its diverse distributional patterns lend themselves well to phylogenetic and biogeographic studies (Brown and Twomey, 2009; Twomey and Brown, 2008), a robust understanding of its evolutionary history is necessary.

Ameerega has a fairly complicated taxonomic and systematic history. The type species, *A. trivittata,* was originally described as *Hyla* by Spix (1824). *Ameerega trivittata* was then transferred to *Dendrobates* (Myers et al., 1978; Silverstone, 1975; Wagler, 1830)*, Hysaplesia* (Schlegel, 1826)*, Hylaplesia* (Knauer, 1878)*, Phyllobates* (Silverstone, 1976), *Ameerega* (Bauer, 1986; Frost et al., 2006; Grant et al., 2006), *Epipedobates* (Myers, 1987), and *Phobobates* (Zimmermann and Zimmermann, 1988). Various other species were assigned to these genera until Grant et al. (2006) transferred the bulk of species in *Epipedobates* to *Ameerega* on the basis of being more closely related to *Colostethus* than to other *Epipedobates.* The nomen *Ameerega* itself was created by Bauer (1986) in his own hobbyist journal and largely ignored until the revision by Grant et al. (2006). After the transfer of the *trans*-Andean *A. andina* and *A. erythromos* to *Paruwrobates* by Grant et al. (2017) and the synonymizing of *A. smaragdina* with *A. petersi* by French et al. (2019), there are currently 30 described species of *Ameerega* (Frost, 2019), though several of these are likely not valid (see Table 1), and instances of additional

undescribed diversity are known (Brown et al., in review). New *Ameerega* species are still being discovered and described, with eight species alone having been described since 2006 (Brown and Twomey, 2009; Lötters et al., 2009; Neves et al., 2017; Serrano-Rojas et al., 2017; Twomey and Brown, 2008; Vaz-Silva and Maciel, 2011).

Species	Authority	Range	IUCN Red List status	Taxonomic status
altamazonica	Twomey and Brown 2008	PE	-	Valid
bassleri	Melin 1941	PE	NT	Valid
berohoka	Vaz-Silva and Medeiros Maciel 2011	BR	LC	Valid
bilinguis	Jungfer 1989	CO, EC, PE	LC	Valid
boehmei	Lötters et al. 2009	BO	LC	Valid
boliviana	Boulenger 1902	BO	LC	Valid
braccata	Steindachner 1864	BR	LC	Valid
cainarachi	Schulte 1989	PE	VU	Valid
flavopicta	Lutz 1925	BR, BO	LC	Valid
hahneli	Boulenger 1884	PE, BR, CO, BO, EC, SU	LC	Valid
ignipedis	Brown and Twomey 2009	PE	LC	Valid
ingeri	Cochran and Goin 1970	CO	DD	Probably rediscovered
labialis	Cope 1874	PE	DD	*nomen dubium*
macero	Rodriguez and Myers 1993	PE, BR	LC	Valid, likely cryptic diversity
munduruku	Neves et al. 2017	BR	-	Valid
parvula	Boulenger 1882	EC, PE	LC	Valid
pepperi	Brown and Twomey 2009	PE	-	Valid
peruviridis	Bauer 1986	PE	-	Likely invalid, synonymous with *trivittata*
petersi	Silverstone 1976	PE	LC	Valid
picta	Tschudi 1838	PE, BR, CO, BO, EC, GU, SU, VE	LC	Valid
planipaleae	Morales and Velazco 1998	PE	CR	Valid
pongoensis	Schulte 1999	PE	VU	Valid
pulchripecta	Silverstone 1976	BR	DD	Valid
rubriventris	Lötters et al. 1997	PE	DD	Valid
shihuemoy	Serrano-Rojas et al. 2017	PE	EN	Valid
silverstonei	Myers and Daly 1979	PE	EN	Valid
simulans	Myers, Rodriguez, and Icochea 1998	PE	LC	Valid
trivittata	Spix 1824	PE, BR, CO, BO, EC, GU, SU, VE	LC	Valid
yoshina	Brown and Twomey 2009	PE	-	Valid
yungicola	Lötters et al. 2005	BO	LC	Likely synonymous with *picta*

Table 1: List of described *Ameerega* species and comments on the taxonomic validity of each. Range abbreviations: PE = Peru, BR = Brazil, CO = Colombia, EC = Ecuador, BO = Bolivia, SU = Suriname, GU = Guyana. IUCN status abbreviations: NT = Near threatened, LC = Least concern, VU = Vulnerable, DD = Data deficient, CR = Critically endangered, EN = Endangered.

Previous phylogenetic reconstructions of *Ameerega* are highly discordant. These discordances may be in part related to the use of different sequence data and/or phylogenetic methods. Early molecular phylogenetic studies including *Ameerega* generally only included a few species and smaller fragments of mitochondrial genes (Clough and Summers, 2000; Santos et al., 2003; Vences et al., 2003, 2000). Later studies included additional taxa and loci, including some nuclear data (Brown and Twomey, 2009; Grant et al., 2006; Roberts et al., 2006; Santos et al., 2009; Twomey and Brown, 2008), with the most recent including around a dozen loci (Grant et al., 2017). The only consistent pattern among topologies is that certain species pairs are generally retrieved as sisters, such as *A. petersi* and *A. cainarachi.* Deeper “backbone” topologies, on the other hand, are liable to considerable fluctuation. The “species groups” to which most taxa are traditionally assigned in the dendrobatid literature are as discordant as the phylogenies, varying between authors in composition and whether they are recognized or not. For example, Lötters et al. (2007) referred *A. bassleri* and *A. silverstonei* to the *trivittata* group based on adult size and morphology. However, Brown and Twomey (2009) found this to be unsupported based on a phylogenetic analysis of mtDNA, and created their own *bassleri* group, consisting of *A. bassleri, A. pepperi, A. yoshina, A. ignipedis,* and *A. pongoensis.* This study did not refer *A. trivittata* or *A. silverstonei* to any species group. Most recently, Grant et al. (2017) maintained the *bassleri* group, but added *A. silverstonei* and *A. berohoka* to it, and moved *A. pongoensis* to the *petersi* group. These discordances may be caused by the use of few and different loci in previous studies, which would increase topological discordance caused by potential incomplete lineage sorting and lead to different conclusions among studies (Brown and Twomey, 2009). Inconsistencies could stem from the use of predominantly mitochondrial DNA in phylogenies, as mitochondrial introgression is suspected to occur in this genus (Brown et al., in review; Brown and Twomey, 2009; French et al., 2019), causing hybrid terminals to be scattered throughout clades containing both parental species.

Other issues in *Ameerega* systematics are the placement of newly described or enigmatic species, and the possibility of cryptic species diversity. Four new species, *A. shihuemoy* Serrano-Rojas et al. 2017, *A. munduruku* Neves et al. 2017, *A.* sp. "Panguana" (Brown et al., in review), and *A.* sp. "Ivochote" (Brown et al., in review) have been described only within the past few years or are currently being described. Serrano-Rojas et al. (2017) provided a mitochondrial 16S phylogeny in their description of *A. shihuemoy,* suggesting that it is sister to a clade composed of *A. macero*, *A. altamazonica* and *A.rubriventris*. *Ameerega munduruku* has not been included in a phylogeny, but its appearance and genetic distances based on 16S sequences suggest an affinity to *A. flavopicta* (Neves et al., 2017). There is strong evidence that *A.* sp. "Ivochote" and *A.* sp. "Panguana" are related to *A. rubriventris* and *A. altamazonica* (Brown et al., in review). The critically endangered Oxapampa poison frog *A. planipaleae* Morales and Velazco 1998, the poorly understood *A. ingeri* Cochran and Goin 1970, and the recently rediscovered *A. boliviana* Boulenger 1902 (Gonzales-Álvarez et al., 1999) have never been included in a phylogenetic analysis due to their rarity. Other putative

Ameerega species are known in the literature but remain undescribed, such as *Ameerega* sp. "PortoWalter1" (see Twomey and Brown, 2008, who found it related to *A. macero*). We include all of these taxa and more in our analyses.

In this study we aim to clarify the evolutionary relationships within *Ameerega* by applying recently developed phylogenomic techniques. Genomic subsampling methods such as sequence capture (Faircloth et al., 2012; Hodges et al., 2007; Lemmon et al., 2012; Okou et al., 2007), RAD-seq (Miller et al., 2007), and transcriptomics (Wang et al., 2009) have recently allowed phylogenetic investigations based on thousands of loci rather than dozens (Lemmon and Lemmon, 2013). One of the most popular established protocols for genome-scale subsampling is the sequence capture of ultraconserved elements (UCEs), which are short sequences of nuclear DNA with nearly 100% identity across a given set of taxa (Bejerano et al., 2004; Faircloth et al., 2012). The regions flanking a UCE are increasingly variable with distance from the ultraconserved core region, making them applicable for phylogenetic analyses across both shallow and deep timescales (Faircloth et al., 2012). By accounting for gene tree discordance using phylogenetic summary methods consistent with the multispecies coalescent (e.g., Liu and Yu, 2011; Mirarab et al., 2014), the species tree can be more accurately estimated. Here we use UCE sequence capture, species tree methods, and divergence time estimation to reconstruct the evolutionary relationships among *Ameerega* species.

2. Materials and Methods

2.1. Sequence acquisition

We acquired 104 tissue samples from field work, museums, and collaborators, accounting for the majority of described *Ameerega* species (Table S1). We included the colostethine dendrobatids *Colostethus pratti* and *Silverstoneia nubicola* as outgroups. When possible, we included multiple samples for each putative species to account for geographic variation and potential cryptic diversity. For each sample, we extracted genomic DNA with the Qiagen DNeasy Blood and Tissue Kit (Valencia, CA, USA) and quantified yield with a Qubit 3 fluorometer (ThermoFisher Scientific). We sent extracted DNA to RAPiD Genomics (Gainesville, FL, USA), where sequence capture and Illumina sequencing of UCEs were performed as per Faircloth et al. (2012). The samples were enriched with the Tetrapods-UCE-5Kv1 set of 5,472 probes, which targets 5,060 UCE loci (Faircloth et al., 2012; Keping et al., 2014).

2.2. Read quality trimming, sequence assembly, and alignment

We performed most of our bioinformatic steps in the software package PHYLUCE v1.5.0 (Faircloth, 2016), a wrapper for several bioinformatic pipelines, as follows. First, we quality-trimmed our raw reads using Illumiprocessor v2.0.6 (Faircloth, 2013), a Python wrapper for the program Trimmomatic v0.36 (Bolger et al., 2014). We used default options in Illumiprocessor, including filtering out bases with a Phred score below 33, and reads below a minimum length cutoff of 40 bp. We assembled the trimmed reads with Trinity v2.0.6 (Grabherr et al., 2011), as implemented in PHYLUCE, using a minimum kmer coverage of 2 (the default value). We used

the phyluce_assembly_get_fastq_lengths.py script to assess assemblies and removed samples with obviously low quality (i.e. below 1,000 contigs).

From here, we created two taxon sets for downstream analyses: one containing all samples (n = 104, “comprehensive dataset”), and the other containing one sample per putative species (n = 35, “restricted dataset”). We created the smaller restricted dataset to increase the computational efficiency of divergence time estimation later on. We defined a putative species (including undescribed ones) based on the comprehensive dataset, which was analyzed first. Putative species were defined by monophyly, with undescribed putative species delineated by expert opinion incorporating geographical, ecological, and morphological characteristics. For each dataset, we mapped contigs to UCE loci using PHYLUCE, retaining those loci which were found at least once in any of the samples within the dataset. We then performed per-locus alignments with MUSCLE v3.8.31 (Edgar, 2004) as implemented in PHYLUCE, with default values including a sliding window size of 20 bp, and a 65% proportion of taxa required to possess sequence at either end of the alignment.

For both datasets, we filtered for matrix incompleteness by only retaining loci present in 70% or more of taxa. We performed additional filtering by calculating the number of parsimony-informative sites (PIS) using PHYLOCH v1.5-5 (Heibl, 2008) within a custom R script. We performed two types of filtering for PIS. First, for downstream concatenated maximum likelihood analyses, we retained loci with 15 < PIS < 100 (for the comprehensive dataset; 1,203 loci retained), and loci with 8 < PIS < 50 (for the restricted dataset; 1,067 loci retained). We set upper limits on the number of PIS to filter out outlier loci, and set lower limits to filter out less-informative loci. We chose PIS limits based on examinations of the distributions of PIS per locus and aimed to retain ~70% of the more-informative loci (while excluding outliers). The comprehensive dataset contained more PIS in general due to the higher number of taxa included, so we used a higher PIS limit to filter that dataset. The alignments for all retained loci from each dataset were concatenated using PHYLUCE. On the other hand, for downstream coalescent analyses, we followed Hosner et al. (2016) in retaining a set of the most-informative loci, in our case retaining the 200 most-informative loci (i.e., the 200 loci with the most PIS) from both comprehensive and restricted datasets, after filtering for 70% matrix completeness.

2.3. Phylogenetic analyses

We performed maximum likelihood (ML) analyses on the concatenated matrices produced by filtering loci for both matrix completeness (70%) and PIS (15 < PIS < 100 for the comprehensive dataset; 8 < PIS < 50 for the restricted dataset). Our ML analyses were performed in IQ-TREE v1.5.5 (Nguyen et al., 2015), using a general time-reversible (GTR) model and assessing support with 10,000 ultrafast bootstrap replicates (Minh et al., 2013). We concatenated the loci into a single alignment and did not partition the matrix due to computational constraints. Additionally, because the nature and function of UCEs in the genome are not well understood and most UCEs are not protein-coding, it is currently unclear whether variable-model partition schemes are appropriate for them (Streicher and Wiens, 2017, 2016; though see Tagliacollo and Lanfear, 2018). We used the results of the large ML phylogeny (Fig. S1) to inform the selection of samples for the restricted dataset (one sample per putative species) as well as for the species tree analyses, where each sample is assigned to a putative species.

In addition to the ML analyses, we performed species tree analyses consistent with the multispecies coalescent using the 200 most parsimony-informative loci from both comprehensive and restricted datasets. Our locus selection for these analyses was greatly restricted due to evidence that removing low-information loci from coalescent summary methods can reduce inference errors due to gene tree bias (Hosner et al., 2016). We also used fewer loci to increase the computational efficiency of downstream Bayesian divergence time analysis. We performed our species tree analyses in ASTRAL-III v5.6.1 (Zhang et al., 2018), a quartet-based gene tree summary method. For the comprehensive dataset, we assigned each sample to one of 35 putative species based on its position in the comprehensive ML phylogeny, and for the restricted dataset we did not make any species assignments, effectively assuming each sample was a separate species. As input for ASTRAL-III, we made separate gene trees for each UCE locus in IQ-TREE, assuming a GTR model and analyzing support with 1,000 ultrafast bootstrap replicates. Because individual UCEs generally have low informative content, near-zero length branches are common in analyses of a single UCE locus, which can bias species tree methods downstream (Meiklejohn et al., 2016). Therefore, we contracted nodes separated by very short branches into polytomies using the *-czb* option in IQ-TREE v1.6.5, an approach recommended by Persons et al. (2016). We used the gene trees as input for ASTRAL, which produced a 35-taxon species tree from both datasets. To assess whether locus selection had a significant effect on topology, we also constructed gene trees from each of the loci in the restricted dataset (after filtering for 8 < PIS < 50; n = 1,067) and used these as input for a separate ASTRAL analysis, using identical IQ-TREE settings and ASTRAL mapping file.

To better understand the degree of gene tree discordance in our analyses, we performed a qualitative visualization of gene trees in DensiTree v2.2.6 (Bouckaert, 2010). However, we had to create a reduced-representation dataset of 10 taxa in order to obtain loci in which all taxa were present, as DensiTree requires taxon completeness in all input trees. We selected one sample from each putative species group (including samples of *A. silverstonei, picta,* and *trivittata,* which are not referred to any species group), which had the most contigs after assembly of all samples in that species group. After filtering this dataset for 100% completeness, we retained 370 loci. We performed maximum likelihood analyses on them in IQ-TREE v1.6.5, using a GTR model with 1,000 ultrafast bootstrap replicates, and setting the outgroup taxon to *A. silverstonei* using the *-o* option to produce rooted trees for clearer visualization. We time-calibrated the trees using the *chronos* function in the R package APE v5.3 (Paradis, 2004), setting the root node calibration to a uniform distribution with bounds equal to the BEAST 2 95% confidence intervals for the node separating *A. silverstonei* from the rest of *Ameerega* (see part 2.4 for details). The time calibration step was intended to produce ultrametric trees with meaningful branch lengths for visualization in DensiTree. We also used the uncalibrated gene trees in an ASTRAL-III analysis to demonstrate that consistent results are achieved despite gene tree discordance and disparities in taxon set.

2.4. Divergence time estimation

For the calibration node in our divergence time estimation, we used an estimate of the divergence of *Colostethus* and *Ameerega* from Santos et al. (2009). The average of the three provided estimates of this node's age was 23.325 Ma, with upper and lower bounds of its 95% credibility interval corresponding to 17.646 and 29.693 Ma. We first used RelTime (Tamura et

al., 2012) to estimate divergence times, which appealed to us because it was designed to be used with large multilocus datasets (Mello et al., 2017), as opposed to the notoriously slow Bayesian methods. We performed divergence time estimation using the RelTime method as implemented in MEGA X v10.0.5 (Kumar et al., 2018), using the filtered and concatenated restricted dataset matrix (1,067 loci), the ASTRAL tree from the restricted dataset as our input tree, the GTR+G+I model with 4 gamma rate categories, and the ancestral node of *C. pratti* and *Ameerega* calibrated as a uniform distribution (the only option in the iteration of MEGA X used) with upper and lower limits at 17.646 and 29.693 Ma.

We compared our divergence time estimates from RelTime with estimates derived from a Bayesian method, BEAST 2 v2.5.0. Because Bayesian methods are computationally demanding, we used the 200 most parsimony-informative loci from the restricted dataset rather than a full-matrix approach. This also allowed for greater consistency with our restricted-dataset ASTRAL starting tree, which was constructed using the same set of loci. We split the 200 loci into four subsets of 50 loci each to further reduce computational demands. We analyzed each subset twice in BEAST 2 in order to ensure that the runs converged. For each analysis, we concatenated each subset and did not partition the alignment, as partitioned alignments can take intractably long periods of time to converge, and may not always produce consistent divergence times (Ješovnik et al., 2017). We used an HKY model with 4 gamma rate categories, with base frequencies set to “empirical”. We avoided the GTR model because it can lead to overparameterization, in turn causing low ESS values (Drummond and Bouckaert, 2015). We used the relaxed lognormal clock model, with a clock rate prior of 1e-10. We obtained this order of magnitude from an estimate of avian UCE substitution rates in Winker et al. (2018). To further reduce computational demands, we did not estimate topology in our analyses and used the restricted-dataset ASTRAL tree as a fixed tree, switching off the subtreeSlide, narrowExchange, wideExchange, and wilsonBalding operators by setting them equal to zero (see Hsiang et al., 2015, who also used this method). We used a Yule tree prior with other priors set to default values. Our calibration constrained the clade including *C. pratti* and *Ameerega* to monophyly and assigned a normal distribution with a mean value of 23.325 Ma and standard deviation of 3.071 Ma to their ancestral node. We ran each analysis with an MCMC chain length of 100,000,000 generations, a log sampling frequency of 100,000 generations and a tree sampling frequency of 10,000 generations. We assessed convergence and ESS values with Tracer v1.7.1 (Rambaut et al., 2018), finding all parameters to have ESS values well over 200, and that, for each subset, parameters converged to similar values after both independent runs. We also used TreeStat v1.2 (http://tree.bio.ed.ac.uk/software/treestat/) to assess whether similar node heights were attained in runs of the same set of loci, and also between different sets of loci, and found that they did. We used LogCombiner v2.5.0 (Bouckaert et al., 2014) to combine the posterior distribution of trees for all runs, accounting for 10% burnin. We then used TreeAnnotator v2.5.0 (Bouckaert et al., 2014) to summarize the resulting tree file, targeting the tree with mean node heights. To assess whether divergence time estimates from more-informative loci differed from those from random loci, we performed an additional BEAST analysis using a concatenated matrix of 200 random loci, using identical BEAUti settings, aside from constraining the analysis to the ASTRAL topology constructed from the full PIS-filtered restricted dataset (rather than the tree constructed from the 200 most informative loci).

3. Results and Discussion

3.1. UCE sequence capture and filtering

For the comprehensive dataset of 104 samples, we recovered 2,685 UCE loci that could be found in at least one sample. After filtering for only loci present in 70% or more of taxa, the dataset was reduced to 1,668 loci. No UCE locus was shared among all 104 taxa. After filtering for 15 < PIS < 100, the comprehensive dataset was further reduced to 1,203 loci. For the restricted dataset with 35 samples, we recovered 2,557 UCE loci. At 70% completeness this was filtered down to 1,692 loci, and after filtering for 8 < PIS < 50 we retained 1,067 loci.

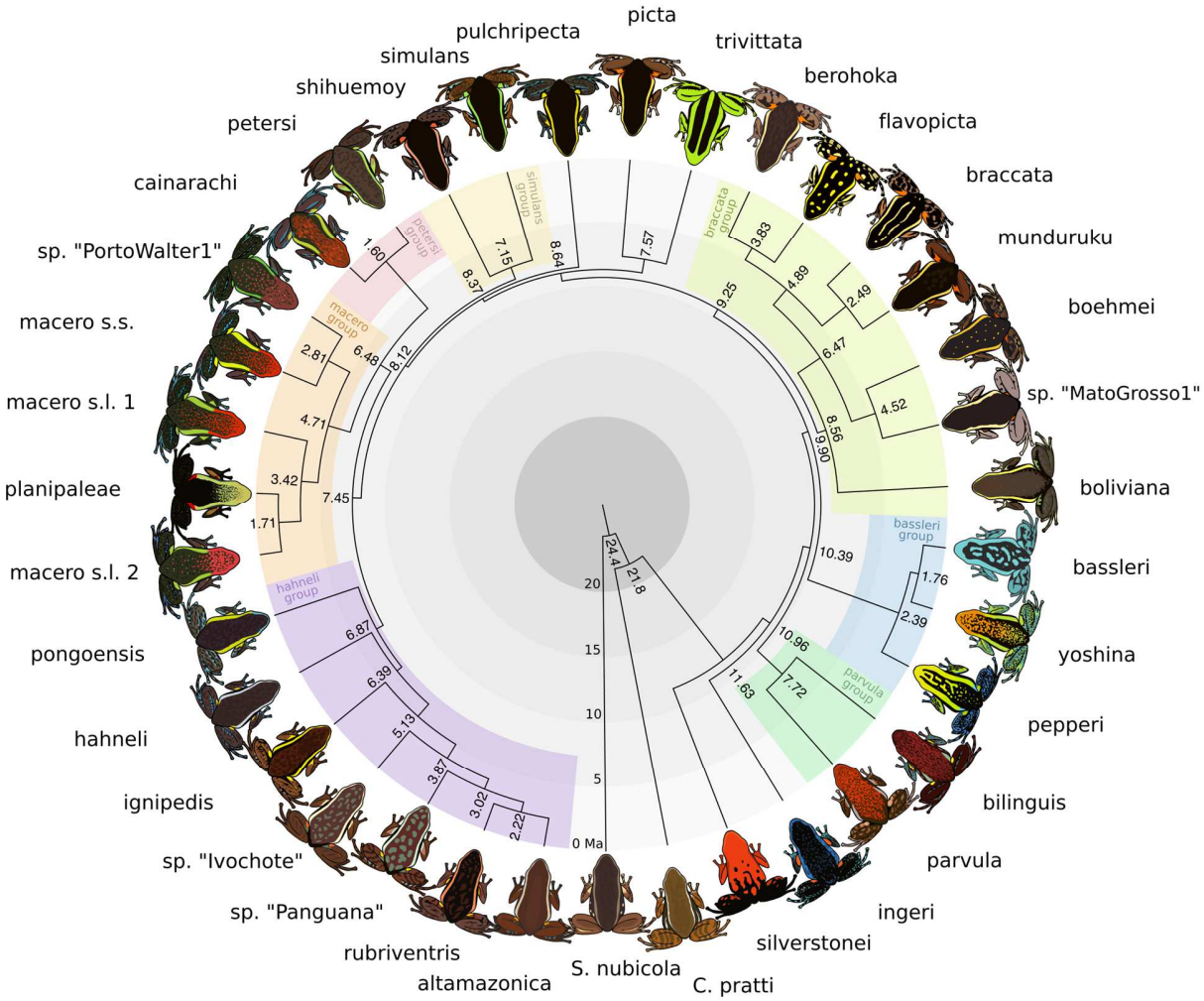

Figure 1: *Ameerega* phylogeny time-calibrated in BEAST 2. The topology was constrained to that of the ASTRAL-III tree recovered from the 200 most parsimony-informative UCE loci for the restricted dataset (see Fig. S2). This consensus tree is the combined result of eight BEAST 2 runs over four datasets of 50 UCE loci each. Node labels are divergence times in millions of

years ago (Ma). Assigned species groups are highlighted and labeled. All illustrations by WXG. **This figure to be printed in color**

3.2. Phylogenetic results

Overall, our phylogenetic results (Fig. 1) differed greatly from previously published estimates of the *Ameerega* phylogeny (Brown and Twomey, 2009; Grant et al., 2017, 2006; Roberts et al., 2006; Santos et al., 2009; Twomey and Brown, 2008). Topologies recovered from different methods (IQ-TREE versus ASTRAL-III, see Fig. S2), datasets (comprehensive versus restricted, see Fig. S3), and filtering schemes (most-informative loci vs. general PIS filtering, see Fig. S4) were similar to each other, with some differences that are expanded upon herein. We found little support for the same species groups previously espoused in the literature (e.g., Brown and Twomey, 2009; Lötters et al., 2007), and propose a new suite of species groups with revised compositions (Figs. 1 and S1). Certain species are not included in these proposed species groups as we have doubts about their legitimacy; see Table 1 for additional details.

Some of the differences between our topologies and those of previous studies are probably due to high levels of gene tree discordance thanks to *Ameerega*'s rapid diversification, leading to short internode branches, which when combined with high effective population sizes can lead to rampant incomplete lineage sorting. Our visualization of gene tree discordance in *Ameerega* (Fig. S5) demonstrates the high level of incomplete lineage sorting in this genus, at least within UCE loci. Despite this discordance, coalescent methods and even concatenation manage to converge on consistent results.

Revised species groups in Ameerega

Ameerega hahneli species group. A monophyletic assemblage of 5 described species: *A. hahneli* (Boulenger, 1884), *A. rubriventris* (Lötters et al., 1997), *A. pongoensis* (Schulte, 1999), *A. altamazonica* (Twomey and Brown, 2008), *A. ignipedis* (Brown and Twomey, 2009).

Ameerega petersi species group. A monophyletic assemblage of 2 species: *A. petersi* (Silverstone, 1976) and *A. cainarachi* (Schulte, 1989).

Ameerega macero species group. A monophyletic assemblage of 2 species: *A. macero* (Rodríguez and Myers, 1993) and *A. planipaleae* (Morales and Velazco, 1998).

Ameerega simulans species group. A monophyletic assemblage of 2 species: *A. simulans* (Myers et al., 1998) and *A. shihuemoy* (Serrano-Rojas et al., 2017).

Ameerega braccata species group. A monophyletic assemblage of 6 described species: *A. braccata* (Steindachner, 1864), *A. boliviana* (Boulenger, 1902), *A. flavopicta* (Lutz, 1925), *A. boehmei* (Lötters et al., 2009), *A. berohoka* (Vaz-Silva and Maciel, 2011), and *A. munduruku* (Neves et al., 2017).

Ameerega parvula species group. A monophyletic assemblage of 2 species: *A. parvula* (Boulenger, 1882) and *A. bilinguis* (Jungfer, 1989).

Ameerega bassleri species group. A monophyletic assemblage of 3 species: *A. bassleri* (Melin, 1941), *A. pepperi* (Brown and Twomey, 2009), and *A. yoshina* (Brown and Twomey, 2009).

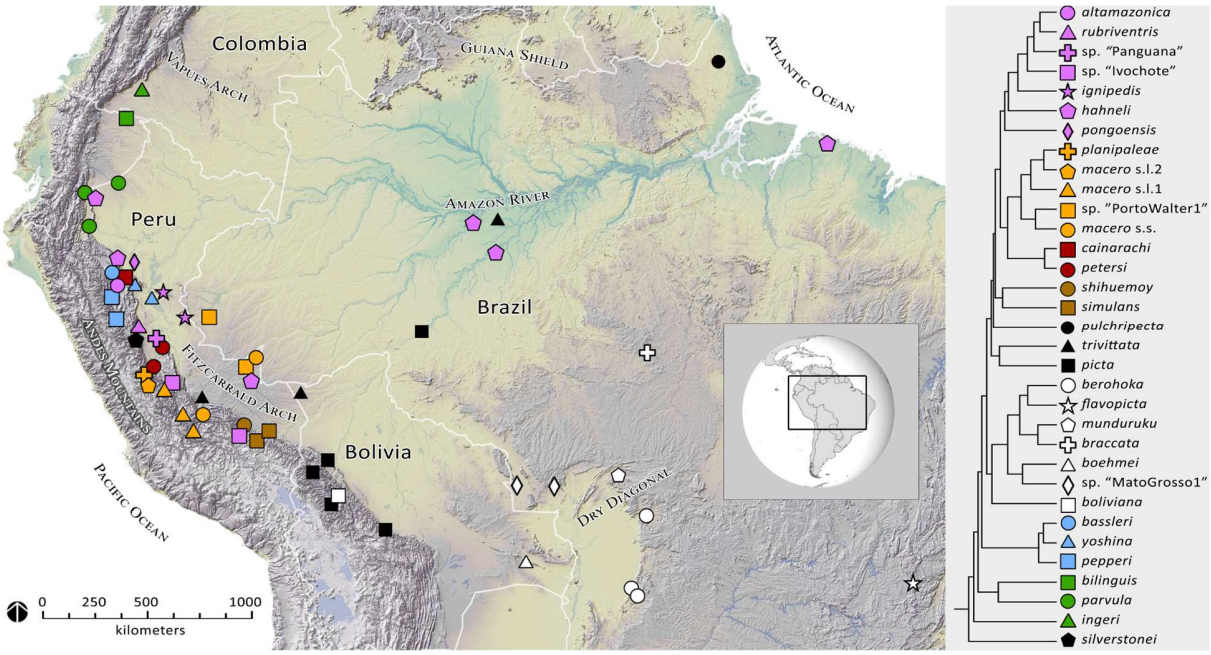

Figure 2: Map of northern South America showing the geographic location of each *Ameerega* sample used in the study. Each type of shape represents a different species, while each color is assigned to groups of similar species (black is assigned to "miscellaneous" species without a species group, and green is assigned to *Ameerega ingeri* and the *parvula* group, which are geographically similar). Also see Fig. S6. **This figure to be printed in color**

3.3. Systematic implications

3.3.1. The hahneli *group*

Ameerega hahneli is a relatively dull-colored species with a black or brown dorsum and white dorsolateral stripes. This species is often confused with other similarly-colored dendrobatids and aromobatids in different parts of its wide distribution, likely due to its morphological conservatism. Twomey and Brown (2008) described the morphologically similar *A. altamazonica* from specimens formerly attributed to *A. hahneli* on the basis of call and genetic differences, restricting *A. hahneli* to lowland Amazonia (Fig. 2). Studies including both taxa (Grant et al., 2017; Roberts et al., 2006; Twomey and Brown, 2008) have not found the two species to be closely related. Here we find that *A. altamazonica* and *A. hahneli* are members of a large clade along with *A. pongoensis, A. ignipedis, A. rubriventris, A.* sp. "Panguana" and *A.* sp. "Ivochote" (Brown et al., in review).

We generally recover *A. altamazonica* as sister to *A. rubriventris,* regardless of the method used (see Fig. S2, though see Fig. S4). Twomey and Brown (2008) also recovered *A.*

altamazonica and *A. rubriventris* as sister species. *Ameerega* sp. "Panguana" is recovered as the sister taxon to these two species, consistent with the findings of Brown et al., (in review). *A.* sp. "Ivochote" is also consistently recovered as sister to the clade containing *A. rubriventris, A. altamazonica,* and *A.* sp. "Panguana". We also include *Ameerega ignipedis* and *A. pongoensis,* two other small frogs with greenish dorsolateral stripes, within the *hahneli* group. *Ameerega ignipedis* has previously been found sister to the *bassleri* group (Brown and Twomey, 2009; Grant et al., 2017), but here we consistently recover it as sister to the clade containing *A. rubriventris, A. altamazonica, A.* sp. "Panguana" and *A.* sp. "Ivochote" with maximal support. *Ameerega pongoensis* has also been found to be related to the *bassleri* group (Brown and Twomey, 2009; Roberts et al., 2006; Santos et al., 2009) or to the *parvula* group (Twomey and Brown, 2008), while Grant et al. (2017) recovered it as sister to *A. smaragdina.* We recover *A. pongoensis* as either the sister taxon to all other members of the *hahneli* group when coalescent methods are used, or the sister taxon of *A. hahneli* when ML methods are used (Fig. S2). Note that both results are characterized by relatively low support (Fig. S2). A recent comparison of mtDNA genomic data and UCE nuclear genomic data (Brown et al., in review) revealed that these incongruencies are likely the result of a historic hybridization event between the shared ancestor of *A. altamazonica*, *A. rubriventris*, *A.* sp. "Panguana", and *A.* sp. "Ivochote", and the ancestor of *A. pongoensis.* Additionally, Brown et al. (in review) recovered *A. ignipedis* as sister to *A. pongoensis* based on an analysis of mtDNA genomic data, this clade being sister to all other members of the *hahneli* group. On the other hand, their UCE results matched our ML topologies. We suggest that such nuclear DNA and mtDNA discordance is indicative of historic hybridization following lineage divergence (Brown and Twomey, 2009; French et al., 2019). The discordance could also be due to incomplete lineage sorting between the mitochondrial genome, which functions as an effective single locus, and the rest of the genome.

3.3.2. The petersi *group*

The *petersi* group is one of the most consistently-recognized species groups in the *Ameerega* literature, traditionally composed of the closely-related species *A. petersi, A. cainarachi,* and *A. smaragdina.* We recover the *petersi* group as sister to the *macero* group, a relationship which has not been found in previous studies. The relationships between *A. petersi, A. smaragdina,* and *A. cainarachi* have historically proved difficult to resolve, but recently *A. smaragdina* was synonymized with *A. petersi* on the basis of acoustic, morphological and genomic analyses (French et al., 2019). Grant et al. (2017) included *A. pongoensis* and *A. simulans* in the *petersi* group, which was not supported by our results.

3.3.3. The macero *group*

We consistently recover a clade consisting of the *macero* and *petersi* groups as sister to the *hahneli* group with very high support (Fig. S2). Most previous studies have found *A. macero* to be sister to a clade containing both *A. altamazonica* and *A. rubriventris* (Brown and Twomey, 2009; Grant et al., 2017; Roberts et al., 2006; Twomey and Brown, 2008). The *macero* group presents previously unrecognized cryptic diversity. *Ameerega macero* sensu stricto (s.s.) is a red-backed frog with yellow dorsolateral stripes that is strikingly similar to the unrelated *A. cainarachi, A. parvula, A. bilinguis,* certain morphs of *A. pepperi* and *A. yoshina, a*nd the aromobatid *Allobates zaparo.* It is sister to a potential undescribed species known in the

literature as “PortoWalter1”, sampled by Janalee Caldwell and team in the 1990s at a single site on the banks of the Juruá River in southwestern Brazilian Amazonia (Fig. 2), and first sequenced by Grant et al (2006). This result is consistent with Twomey and Brown (2008) and Grant et al. (2017).

These two putative species are sister to a clade consisting of two separate lineages of *A. macero* sensu lato (s.l.) and the critically endangered *A. planipaleae. Ameerega planipaleae* is substantially different from *A. macero* in terms of its habitat (being more montane, occurring at altitudes as high as 2200 m), appearance, and call, so there is little evidence that this species is a junior synonym of *A. macero*, which would effectively make the *macero* group one monophyletic species. Given the spatial mixing of lineages, each containing a described taxon that appears to be valid, our phylogenetic results suggest a potential role for introgression and hybridization in this complex. One potential explanation is where the common ancestor to *A. macero*, *A.* sp. “PortoWalter1”, and *A. planipaleae* diverged into two lineages of proto-*macero* red frogs and one lineage further diverged into two daughter species in the Andean foothills: *A. planipaleae* and the ancestor of *A. macero* sensu lato. The common ancestor of *Amereega macero* sensu stricto and *A.* sp. “PortoWalter1” simultaneously radiated from the foothills of the Andes across the Fitzcarrald Arch into western Brazil. These deep lineages of *A. macero* (lineage 1: *A.* macero s.s. and *A.* sp. “PortoWalter1”; and lineage 2: *A. macero* s.l. 1) diverged in isolation. However, after a period they came back into contact, interbred, and the two putative daughter species of *macero*-like frogs collapsed, rendering *A. macero* paraphyletic with regard to *A. planipaleae* (this is identical to the scenario suggested by Brown and Twomey (2009) to explain the paraphyly of *A. petersi* by *A. cainarachi*). This group’s evolutionary history seems to be further complicated by secondary hybridization of the ancestors of *A. macero* s.l. 1 and *A. planipaleae,* which could have resulted in the creation of *A. macero* s.l. 2. Cursory examination of specimens representing all *A. macero* lineages and *A.* sp. “PortoWalter1” reveal no apparent morphological differences (JLB, unpub. data). This group requires further study to clarify the systematic relationships and specific status of *A. sp.* “Portowalter1”*, A. macero* s.l. *1*, and *A. macero* s.l. *2,* and how they relate to *A. macero* s.s. and *A. planipaleae.*

3.3.4. The simulans *group*

We consistently recover *A. shihuemoy,* which was described in 2017 by Serrano-Rojas et al., as sister to *A. simulans,* and place both species in the *simulans* group. Serrano-Rojas et al. (2017) found *A. shihuemoy* to be most closely related to *A. macero, A. altamazonica,* and *A. rubriventris* based on 16s mitochondrial data. We find the *simulans* group itself to be sister to the clade containing the *macero, petersi,* and *hahneli* groups, with relatively low-to-high support (Fig. S2). Other authors have found *A. simulans* to be part of or sister to the *petersi* group (Grant et al., 2017; Santos et al., 2009), though other estimates vary (Brown and Twomey, 2009; Roberts et al., 2006; Twomey and Brown, 2008).

3.3.5. The braccata *group*

We recover the *braccata* group as sister to a clade composed of the previously discussed groups, as well as *Ameerega trivittata, A. picta,* and *A. pulchripecta.* Frogs in the *braccata* group are morphologically similar, with a dark brown to black dorsum, white to yellow dorsolateral stripes, and the varying presence of dorsal spots or blotches (Fig. 1). Uniquely

among dendrobatids, most of the frogs in this group inhabit the seasonal Cerrado savannahs from central Brazil to Bolivia (Fig. 2). Previous analyses of this group have been incomplete, generally limited to finding *A. braccata* and *A. flavopicta* to be sister species (Brown and Twomey, 2009; Grant et al., 2017; Santos et al., 2009). Placement of the group itself within the *Ameerega* phylogeny has varied between studies.

The recently described *A. munduruku* (Neves et al., 2017), a species previously considered conspecific with *A. picta* but not included in a phylogenetic analysis before, was found to be sister to *A. braccata. Ameerega munduruku* is the only species in the *braccata* group found in wet forest environments; it occurs on rocky outcrops within southern Brazilian Amazonia on the banks of the Teles Pires River (a tributary of the Tapajós) (Neves et al., 2017; Prates et al., 2012) (Fig. 2). We found the clade composed of these two species to be sister to a clade composed of *A. flavopicta* and *A. berohoka,* the latter being another recently described Brazilian species (Vaz-Silva and Maciel, 2011) (Fig. S2). In the case of the ASTRAL tree derived from loci with 8 < PIS < 50, A. flavopicta and A. berohoka were nonmonophyletic (Fig. S4).

The four aforementioned taxa are recovered as sister to another clade consisting of *A. boehmei* and a yet-undescribed species, here called sp. “MatoGrosso1”. This unnamed species was sampled in western Brazilian cerrado (state of Mato Grosso), close to the Bolivian border (Fig. 2). These specimens were tentatively assigned to the Amazonian species *A. picta*, but our results suggest that these two species are not closely related in spite of their morphological similarity. As for *A. boehmei*, Grant et al. (2017) found this species to be sister to the clade containing *A. braccata* and *A. flavopicta,* which overall is consistent with our results given that they only included those three taxa from this species group.

We also place *A. boliviana,* which was rediscovered in 1999 after not having been seen for nearly a century (Gonzales-Álvarez et al., 1999), in a phylogeny for the first time, recovering it as the sister taxon to the rest of the *braccata* group. The placement of this species may indicate a Bolivian origin for the *braccata* group, and lends credence to the initial radiation of *Ameerega* occurring in the Andes.

3.3.6. The bassleri *group*

The *bassleri* group is composed of three phenotypically variable species from the eastern Andean foothills of central Peru: *Ameerega bassleri, A. pepperi,* and *A. yoshina.* Our placement of the *bassleri* group is variable, along with that of the *parvula* group. When the 200 most informative loci are used, the *bassleri* group is recovered as sister to the clade containing all previously discussed *Ameerega* species (the *hahneli, macero, petersi, simulans,* and *braccata* groups, plus *A. trivittata, A. pulchripecta,* and *A. picta*), and the *parvula* group is sister to all of these plus the *bassleri* group (Figs. 1, S2). When all loci are used (after standard completeness and PIS filtering), the *bassleri* and *parvula* groups effectively switch places, with the *bassleri* group moving closer to the root node of the *Ameerega* phylogeny (Figs. S1, S3, S4). Both methods recover these topologies with relatively low node support (Fig. S1, S2, S3, S4). These incongruencies are suggestive of a rapid radiation with the resulting short internodes; indeed, our BEAST 2 results suggest the *bassleri* and *parvula* groups are only separated by a divergence of ~500,000 years (see Table S2).

Within the *bassleri* group, we consistently recover *A. pepperi* as sister to the clade containing *A. bassleri* and *A. yoshina,* similar to the analysis from the original description of *A. pepperi* and *A. yoshina* (Brown and Twomey, 2009), but differing from Grant et al. (2017), who recovered *A. pepperi* and *A. yoshina* as sister species. Our results in terms of the overall composition of the *bassleri* group do not agree with those of Brown and Twomey (2009), who included *A. ignipedis* and *A. pongoensis* in this group, or of Grant et al. (2017), who included *A. silverstonei, A. berohoka,* and *A. ignipedis.*

3.3.7. The parvula *group*

We place the species *A. parvula* and *A. bilinguis,* found to be sister in our analyses, in the *parvula* group. These two frogs have historically been thought to be closely related, but are not always recovered as sister taxa (see Grant et al., 2017; Santos et al., 2009). As discussed in the previous section, our placement of the *parvula* group is inconsistent (see Fig. S2), likely due to rapid lineage divergence that made the resulting short internodes difficult to resolve, as well as discordance in dataset resulting from filtration method. Previous studies have recovered these frogs as sister to (Brown and Twomey, 2009; Roberts et al., 2006) or part of (Twomey and Brown, 2008) the *bassleri* group, or even sister to the entire genus *Ameerega* (Grant et al., 2017; Santos et al., 2009).

3.3.8. Other Ameerega *species*

The species *A. trivittata, A.picta,* and *A. pulchripecta* formed a clade in ML (see Figs. S1 and S2) but not in coalescent-based analyses (see Figs. S2, S3, S4). They are characterized by near-zero-length internode branches, which probably contributes to the observed ambiguity and discordance between methods and datasets. Collectively, these species are nonetheless consistently recovered as sister to a clade composed of the *simulans, petersi,* and *hahneli* groups. In the ASTRAL tree constructed from the restricted dataset and most-informative loci (Fig. S2), *A. trivittata* and *A. picta* form a clade (albeit with low support). With our current results we cannot say definitively what the true relationships are among these species or between them and the other species of *Ameerega.* Given the discordance between methods, we do not assign them to any particular species group; if upon further investigation the monophyly of these three species is borne out (as in Fig. S1), they could be assigned to a *trivittata* group.

Ameerega trivittata, among the largest dendrobatids, has been known to contain little genetic structure despite its wide distribution across the Amazon Basin from Guyana to Peru and northern Bolivia (Fig. 2) (Roberts et al., 2006). We also find that our *A. trivittata* samples are separated by very short branches (Fig. S1), despite being selected from localities throughout the species' range. We do not find any evidence of cryptic species within this taxon, though significant variation in color and pattern exists (Lötters et al., 2007). There is great inconsistency in the placement of this species in previous studies. We are the first to recover it as sister in any capacity to *A. picta.*

Ameerega picta is another widespread species, to which dendrobatoid specimens have often been misattributed due to having similar coloration. It is similar in appearance to the unrelated *A. munduruku, A.* sp. "Ivochote", *A.* sp. "Panguana", *A. shihuemoy, A. berohoka, A. altamazonica,* and *A. hahneli* (Fig. 1), as well as to the aromobatid *Allobates femoralis*. We find that *A. picta* is paraphyletic with respect to *A. yungicola* (Fig. S1; see samples 0486 and 0790);

we propose that the latter species is a junior synonym of *A. picta*, based on our genetic results and the lack of strong morphological differences. Alternatively, *A. picta* could represent a complex of several cryptic species. Until additional data are collected we cannot properly evaluate either of these hypotheses. Like *A. trivittata,* the exact placement of *A. picta* in previous phylogenies is highly inconsistent.

Ameerega pulchripecta is much more range-limited than *A. trivittata* or *A. picta,* being endemic to northern Brazil (state of Amapá) near the border with French Guiana (Fig. 2). Our placement of this species is highly inconsistent due to apparent rapid cladogenesis at this stage of Ameerega evolution, as indicated by extremely short internodes (Fig. 3; nodes 8-10). When it forms a clade with *A. trivittata* and *A. picta,* it is sister to the clade containing the latter two species (Figs. S1 and S2). In the ASTRAL trees from the restricted dataset, *A. pulchripecta* is sister to the clade containing the *macero, simulans, petersi,* and *hahneli* groups (Fig. S4). In the ASTRAL tree from the comprehensive dataset, on the other hand, *A. pulchripecta* is sister to this clade plus *A. trivittata* and *A. picta* (Fig. S3).

The mysterious Colombian *Ameerega ingeri* was originally described from museum specimens by Cochran and Goin (1970) but has not been seen in the wild for many years as no population could be attributed to the specimens. Recently discovered populations of dendrobatids from sites adjacent to the type locality of *A. ingeri* are morphologically consistent with Silverstone's 1976 description: a large *Ameerega* with a granular dorsum, no dorsolateral stripes, and black dorsum in preserved samples (which is the color that many blue frogs acquire in preservative) (see Lozano, 2015). No other described *Ameerega* species in this area has a similar phenotype, and herein we refer to these samples as *A. ingeri*. We consistently recover *A. ingeri* as sister to the clade containing all other *Ameerega* outside of *Ameerega silverstonei* (Figs. S2, S3), except for the case of the ASTRAL tree from all loci (after filtering for PIS) in the restricted dataset (Fig. S4), where it is sister to all Ameerega outside of A. silverstonei, the bassleri group, and the parvula group. *A. ingeri* does not appear to have any close relatives within *Ameerega* and may represent a relictual lineage from the genus' initial expansion.

Finally, *Ameerega silverstonei* was always recovered as the sister species to the rest of *Ameerega,* no matter the method or dataset used. *Ameerega silverstonei* is a large and distinctive red and black frog (Fig. 1) found in the higher-elevation cloud forests of the Cordillera Azul of Peru (Fig. 2). This species is similar to the members of the *bassleri* group in terms of its advertisement call, range, and limited endemism, but does not appear to be closely related to them.

There are several taxa attributed to the genus *Ameerega* that appear to be invalid and have not been properly discussed elsewhere. The first of these is *Ameerega peruvirids,* described by Luuc Bauer in 1986 (Bauer, 1986), with its type locality "in the Ucayali drainage of East Andean Peru". This taxon is a morph of *A. trivitatta* that was elevated to specific status. A previous analysis by Roberts et al. (2006) and our results include *A. trivittata* from the Ucayali drainage that match the phenotype of the frogs described in Bauer (1986), which suggests that this species is a junior synonym of *A. trivitatta*. However, because the description fails to mention an adequate type locality ("the Ucayali drainage" is quite vague and refers to a very large area) and a holotype is not specified or known to exist, it is exceedingly difficult to confidently ascribe any specific population of *A. trivittata* to Bauer's description. As a result, here we formally classify *A. peruviridis* as a *nomen dubium*.

With regards to *A. labialis,* described by Edward Drinker Cope (1874), we support the conclusion of Lötters et al (2007) that it be classified as a *nomen dubium* based on the notable brevity of the species description, and the fact that the only known specimen, the holotype, has been lost. Both factors make it almost impossible to distinguish the described frog from similar frogs, as well as the lack of images of this frog in life. Lastly, no frogs have been found nearby the type locality of Nauta, Peru that match Cope's limited description.

Ameerega maculata was allocated to the genus *Ameerega* (Grant et al., 2006) based mostly on the existence of maxillary and premaxillary teeth, the first finger being longer than the second, and basal webbing occurring between toes II-IV. *Ameerega* shares these traits with the genus *Epipedobates.* In 2017, Grant et al. provisionally transferred A. maculata to the genus Epipedobates, which we support here. *A. maculata* shares several characteristics with *Epipedobates*, including a *trans*-Andean distribution (vs. *cis*-Andean for *Ameerega*), smooth dorsal skin (though we agree with Myers' (1982) conclusion that granulation can be lost in preservation), and a spotted dorsum, lacking dorsolateral and oblique lateral stripes (as observed in *Epipedobates darwinwallacei*). Given the existence of only a single observation/specimen, we share the skepticism of Lötters et al., (2007) regarding the validity of the type locality of *E. maculata*, given as "Chiriqui" in Panama. Moritz Wagner, the collector, also extensively traveled Ecuador during these trips, which is the core range of *Epipedobates*. Thus, there is a chance that the specimen collection locality was confused at some point prior to the description of this species.

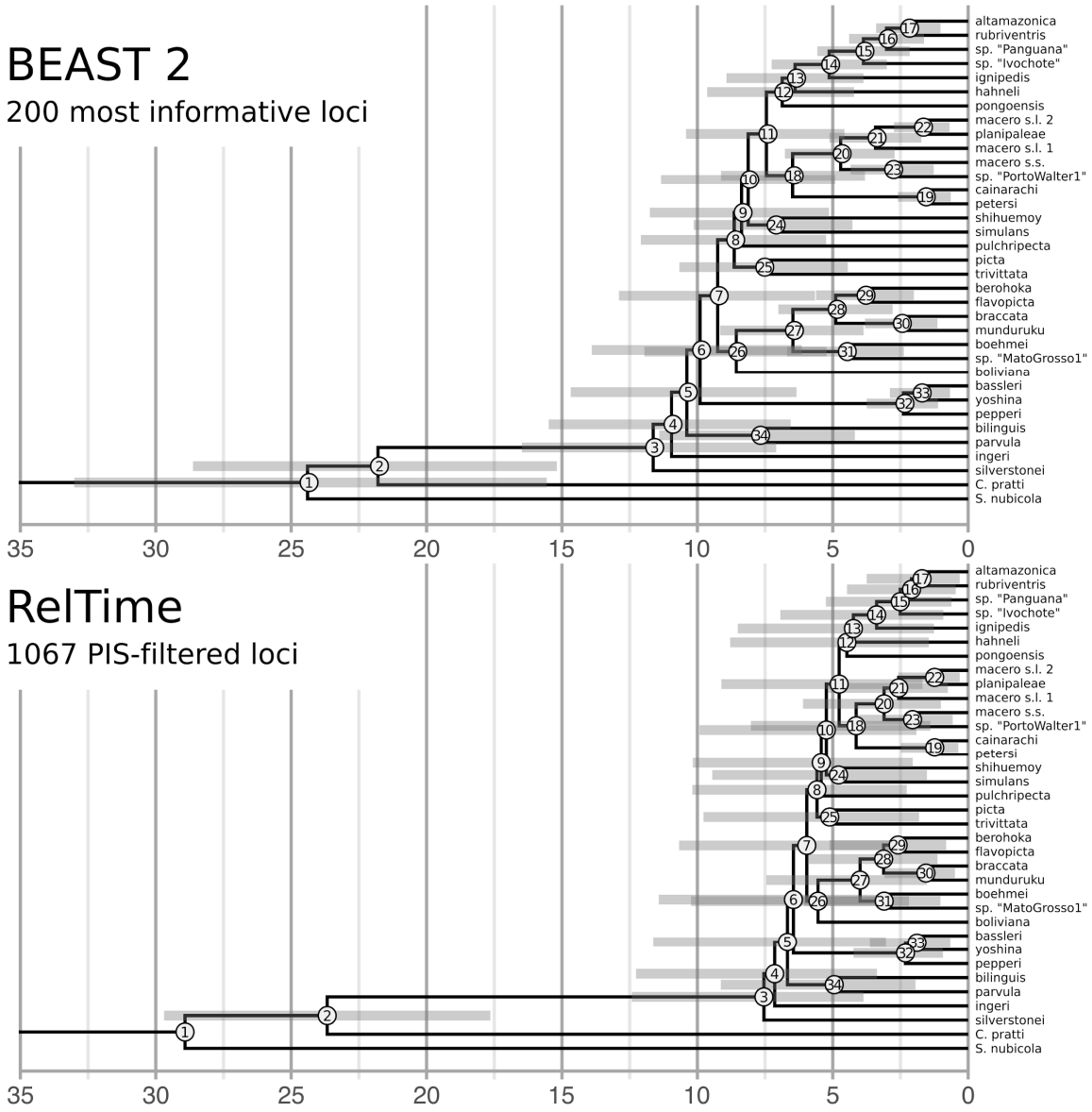

Figure 3: Comparison of the divergence times estimated with BEAST 2 and RelTime (MEGA X). Error bars, shown in gray, represent 95% highest posterior density intervals (in the case of BEAST 2) or 95% confidence intervals (RelTime). Both scale bars are in units of millions of years ago (Ma). Each node is assigned a number which is referenced in Table S2, where we provide exact values for node heights and error bar estimates. Both analyses were calibrated by Node 2. Both topologies are identical to the ASTRAL-III restricted dataset topology constructed from the 200 best loci (Fig. S2). The BEAST 2 tree is identical to the tree displayed in Fig. 1.

3.4. Divergence time estimation

Time-calibrating the dendrobatid phylogeny has proved to be challenging, but is important for contextualizing the evolution of dendrobatids in the geographic history of Latin

America. The main source of uncertainty is the lack of any described dendrobatid fossils, as fossil taxa are one of the most relied-upon methods for calibrating phylogenies (Ho and Duchêne, 2014). The only previous study to make a serious attempt to specifically date the dendrobatid tree is Santos et al. (2009). Santos et al. first made a time-calibrated phylogeny spanning Amphibia using both paleographic and fossil constraints, as amphibians in general have a voluminous fossil record. They then used their divergence time estimate for the split of Dendrobatidae from the rest of Hyloidea as their primary time constraint on the root node of Dendrobatidae. Santos et al. estimated that Dendrobatidae split from Aromobatidae ~40 Ma. We used their divergence time estimation for the split of *Ameerega* from *Colostethus,* around 23 Ma, as our own calibration for this node.

Another challenge in our divergence time analysis was the intractability of our large UCE dataset when using conventional dating methods. The most widely used and accepted programs for divergence time analysis are Bayesian phylogenetics programs such as BEAST (Bouckaert et al., 2014) and MrBayes (Huelsenbeck and Ronquist, 2001). While powerful, these methods are computationally intensive and time-consuming due to the resources required to adequately sample the posterior distribution of trees. In the current age of phylogenomics, where phylogenetic analyses are commonly run on matrices consisting of hundreds of taxa, each with thousands of loci and millions of base pairs, Bayesian analyses can quickly become intractable. We took a dataset-reduction approach to our analysis in BEAST 2, only using 200 loci. However, we were also interested in less computationally-intensive methods that would allow us to use our full dataset. To that end, we compared our BEAST 2 outputs with results from the maximum likelihood method RelTime (Figs. 3 and S7) (Tamura et al., 2012). RelTime was designed for use with large genomic datasets (Mello et al., 2017; Tamura et al., 2012), but has caused controversy in the literature due to one study suggesting that its method converges to a strict clock (Lozano-Fernandez et al., 2017; see Battistuzzi et al., 2018 and Tamura et al., 2018 for responses). The computational difference was readily apparent, as BEAST 2 required roughly 4,275 CPU-hours to process four 50-locus datasets twice, while RelTime required only 19 CPU-hours to process the full 1,067-loci.

While credibility intervals in our results largely overlap, the median divergence times inferred by BEAST 2 and RelTime are quite distinct for certain nodes (Fig. 3 and Table S2). BEAST 2 recovered a stem age for *Ameerega* (i.e., the divergence between *Ameerega* and *Colostethus*) of ~22±7 Ma and a crown age for *Ameerega* (i.e., the divergence between *A. silverstonei* and the rest of the genus) of ~11±5 Ma. By comparison, RelTime pushed the stem age back (~23±6 Ma) and the crown age forward (~7±4 Ma), effectively recovering a much longer branch between the root and crown nodes (Fig. 3). For nodes within *Ameerega,* RelTime recovered divergence dates a full 2 Ma younger than BEAST 2, on average. Given that we used a secondary calibration from their study, our *Ameerega* divergence times are fairly similar to those of Santos et al. (2009). Their estimate for the stem node of *Ameerega* was ~23±6 Ma, and ~8±3 Ma for the crown node.

We also compared divergence time estimates from BEAST 2 analyses on the 200 most informative loci and on 200 random loci to assess whether using the most informative loci only biased the divergence times (Fig. S7). Both of these estimations resulted in overall very similar divergence times; nodes in the latter tree were estimated to be on average 42,000 years older

than in the former, a small amount when considering a timescale of tens of millions of years. This suggests that locus informativeness had little overall effect on divergence time estimation.

While there is no effective way to test the relative accuracy of BEAST 2 or RelTime with our dataset, we base most of our discussion on the BEAST 2 tree (shown in Figure 1) due to the method's wider acceptance in the literature and the increased clarity of interpretation from its larger internode distances. However, the limitations of BEAST 2 and other Bayesian methods are evident when one considers that we were only able to analyze a small portion of our data in BEAST, while using RelTime allowed us to use all of it. We recommend a measured approach to future divergence time estimation studies, as a balance must be struck between data coverage and computation time.

Our divergence time estimation illustrates some of the challenges that have haunted *Ameerega* phylogenetics for nearly two decades. Many internal branches along the "backbone" of the phylogeny are very short, suggesting a rapid radiation of the genus. This is in accordance with Santos et al. (2009), who found that the diversification rate increase associated with Ameerega is the highest in Dendrobatidae. Without large amounts of data, resolving nodes separated by these short branches consistently has historically been very difficult, resulting in the discordance of previous phylogenies. We consistently resolve many backbone nodes in the *Ameerega* phylogeny, such as the relationships between the *hahneli, macero, petersi,* and *simulans* groups, but others remain puzzling, especially the relationship between the *parvula* and *bassleri* groups, which may have diverged from their common ancestor in as little as 2-500,000 years (Table S2). Reconstructing the evolutionary history of *Amereega* is further complicated by the apparent hybridization and introgression between many *Ameerega* species (Brown et al., in review; Brown and Twomey, 2009; French et al., 2019). Future phylogenetic studies of dendrobatid frogs will benefit from the incorporation of methods that attempt to detect and quantify introgression on the basis of genome-scale data (Solís-Lemus and Ané, 2016; Zhu and Nakhleh, 2018).

3.5. Implications for the biogeography and phenotypic evolution of Ameerega

Our newly inferred topology of *Ameerega* provides insights on the history of landscape occupation during the genus' diversification. We consistently recover *A. silverstonei,* localized to the highlands of east-central Peru (Fig. 2), as the sister taxon to the ancestor of all other *Ameerega* species. The next clades to diverge (from the root towards the tips) are *Ameerega ingeri* (southwestern Colombia), the *parvula* group (Ecuador and northeastern Peru), and the *bassleri* group (east-central Peru; note that in our ML analyses the *bassleri* group diverges before the *parvula* group) (Fig. 2). Each of these clades, as well as several lineages in more recently-diverged groups (e.g., the *A. rubriventris* and *A. macero* complexes), is localized to the eastern versant of the Andes (Fig. 2). Their common ancestors' proximity to the root node of *Ameerega* is consistent with the well-established hypothesis of an Andean origin for this genus (Brown and Twomey, 2009; Santos et al., 2009). The radiation of the *Ameerega* crown group (Fig. 3; node 3 onwards) most likely occurred very quickly throughout the northern Andes in the late Miocene (~7-11 Ma; see Fig. 3), potentially coinciding with the tail end of an intense period of Andean orogeny that occurred ~12 Ma (Hoorn et al., 2010). While our BEAST results, which

place the crown group's origin at ~11 Ma, do suggest that contemporaneous Andean uplift had an effect on radiation in this group, our RelTime results, which place the crown group's age at ~7 Ma, instead suggest that the response was delayed by several million years. The uplift of the Andes is known to have had a large effect on dendrobatid evolution (Santos et al., 2009) and on Amazonian biodiversity in general (Hoorn et al., 2010; Rull, 2011). Furthermore, our divergence time estimates suggest that *Ameerega* diversified to the west of potential marine incursions and more recent mega-wetlands such as the hypothesized "Acre system" that existed in northwestern South America at the time, between the Andes and the nascent Amazon rainforest in the east (Hoorn, 1994, 1993; Hoorn et al., 2010; Latrubesse et al., 2010). These environments may have acted as a barrier to dispersal to *Ameerega,* resulting in the relatively low diversity of *Ameerega* species that exist in the present-day Amazon basin and in northern South America.

The disjunction between *A. silverstonei* and *A. ingeri* (Fig. 2)*,* the two most basal and divergent taxa, is suggestive of these species being relictual lineages leftover from the genus' original diversification. The notion of a montane, Andean origin conflicts with the results of Roberts et al. (2006), who used ancestral state reconstruction and divergence-vicariance analysis (DIVA) to support a lowland origin for *Ameerega* and a single highland colonization in northern Peru. That result was most likely due to the topology recovered by Roberts et al., which is essentially the inverse of our topology, with the lowland *A. hahneli* as the sister taxon to all other *Ameerega.* The findings of Brown and Twomey (2009) were more consistent with ours, in that their DIVA analysis suggested that the *bassleri* group had a montane origin.

The *braccata* group, which occupies the "dry diagonal" of cerrado and serranía from central Brazil to Bolivia, demonstrates an unusual distribution for anurans, and especially for dendrobatids. *Ameerega boliviana* is the sister taxon to the rest of the *braccata* group, and exhibits a distribution in the Andes of western Bolivia (Fig. 2). This suggests an Andean origin for the *braccata* group, with *A. boliviana's* position in the phylogeny suggesting that it is yet another relictual lineage from *Ameerega's* original Andean expansion. From the *braccata* group phylogeny, it appears that these frogs continually spread eastward through the dry diagonal, with *A. boehmei, A. sp.* "MatoGrosso1," and *A. braccata* being geographically closest to *A. boliviana,* and *A. munduruku* and *A. flavopicta* the furthest away (Fig. 2). *A. munduruku* itself now occupies the Brazilian Amazon rather than the dry diagonal. This pattern of eastward range expansion from the Andes through the dry diagonal has been observed once before in anurans, in the strabomantid genus *Oreobates,* which is also thought to have an Andean origin with a subsequent spread through the dry diagonal to eastern Brazil (Padial et al., 2012). In accordance with our previous suggestion that the presence of megawetlands in the late Miocene limited the dispersal of *Ameerega* into what would become lowland Amazonia, it is possible that the ancestors of the *braccata* group were forced to disperse into this area by the presence of such inhospitable wetland environments to the north.

The presence of *A. silverstonei* and the *bassleri* and *parvula* groups, all of which are brightly-colored frogs (Fig. 1), near the base of the *Ameerega* phylogeny also suggests that the ancestral *Ameerega* was brightly-colored. In contrast, the most closely related genera to *Ameerega* (*Colostethus* and *Leucostethus;* (Grant et al., 2017; Guillory et al., 2019)) are both composed solely of relatively dull, black- or brown-colored species. In fact, the only other representatives of the subfamily Colostethinae that are brightly-colored are some species of

Epipedobates. Further testing is required to confirm this pattern of phenotypic evolution, and more studies should focus on the evolution of aposematism in colostethines. Our suggestion that the ancestral Ameerega was possibly aposematic conflicts with the findings of Roberts et al. (2006), who, based on an ancestral state reconstruction, suggested that the ancestral *Ameerega* was not aposematic, again likely due to the presence of the cryptically-colored *A. hahneli* as the sister taxon to the rest of the genus in their phylogeny. The implication of our result is that bright coloration (and probably aposematism) was present in the ancestor of *Ameerega* and was subsequently lost and regained several times (e.g. in the *braccata, petersi,* and *macero* groups).

Another interesting pattern apparent from our phylogeny is the convergent evolution of several phenotypic syndromes. For example, there are seven described species of *Ameerega* with bright red dorsa (this includes certain morphs of *A. yoshina* and *A. pepperi*) and there are six species with bright green or yellow dorsolateral lines, often with matching ventrolateral coloration, paired with a dark-colored dorsum. In most cases these taxa are unrelated, suggesting that similar species may be involved in Müllerian mimicry similar to that of other poison frogs (Symula et al., 2002). However, this is likely a case of "mimicry without models" (Pfennig and Mullen, 2010), as there are no known cases of sympatry between putative mimics (see, for example, the disjunction between members of the *macero* group and the similarly-colored *A.* cainarachi). The possibility of Batesian mimicry can also not be discounted until more detailed study on *Ameerega* toxicity and/or unpalatability is completed. In general, the advergence of aposematic coloration is known to have an adaptive benefit via the reduction of necessary predator learning required to distinguish between species, as observed in the dendrobatid genus *Ranitomeya* (Twomey et al., 2016).

4. Concluding remarks

Based on extensive sampling of taxonomic and genomic diversity, our investigation offers a new phylogenetic framework for the poison frog genus *Ameerega*. Our inferred topology is markedly different from those proposed by previous investigations, with fundamental implications for the group's taxonomy, biogeography, and phenotypic evolution. The results also pose a range of questions to be addressed by future studies. These include, for instance, the role of adaptation during the invasion of open and dry habitats by the *braccata* species group; the evolutionary causes and implications of repeated reduction or loss of aposematic coloration in *Ameerega*; the possibility of Müllerian mimicry between similar co-distributed species; and the consequences of hybridization and genetic introgression for speciation and phenotypic diversification in the genus. Our results also point to unrecognized diversity in *Ameerega*, which we hope will support future taxonomic revisions and, if warranted, the description of new species.

5. Acknowledgements

We thank Miguel T. Rodrigues (Universidade de São Paulo), Felipe F. Curcio (Universidade Federal do Mato Grosso), Jose Padial (Museo Nacional de Ciencias Naturales - Madrid), and Diego J. Santana (Universidade Federal do Mato Grosso do Sul) for providing

tissue samples under their care. IP acknowledges funding from a Smithsonian Peter Buck Postdoctoral Fellowship. Much of this research was supported by start-up to JLB provided by SIU. WXG is thankful for funding from the Students United in Exploring, Preserving, and Researching Biodiversity (SUPERB) fellowship, funded by the US National Science Foundation (NSF). We thank César Aguilar (MUSM) and Greg Schneider (UMMZ) for allowing access to specimens under their care. IDIR thanks the Spanish government for funding under project CGL2014-56160-P. Permits were issued by: Brazil's Instituto Chico Mendes de Conservação da Biodiversidade issued sample collection and transport permits (SISBIO 30309, 36753, 7147) the Servicio Nacional Forestal y de Fauna Silvestre in Peru (R.D.G. 120-2012-AG-DGFFS-DGEFFS, R.D.G. 029-2016-SERFOR-DGGSPFFS, R.D.G. 405-2016-SERFOR-DGGSPFFS, R.D.G. 116-2017-SERFOR-DGGSPFFS, N° 002765-AG-INRENA, N° 061-2003-INRENA-IFFS-DCB, N° 050-2006-INRENA-IFFS-DCB, N° 067-2007-INRENA-IFFS-DCB, N° 083-2017-SERFOR/DGGSPFFS, N°004-2013-SERNANP-JRCA, and N°016-2010-SERNANP-DGANP), Contrato de Acceso Marco a Recursos Genéticos in Peru (359-2013-MINAGRI-DGFFS-DGEFFS, and Ministerio de Agricultura of Peru (Permit Number Code 25397, N° 2904-2012-AG-DGFFS-DGEFFS) and the administration of Manu National Park (06-2013-SERNANP-PNM-JEF).

References

Bauer, L., 1986. A new genus and a new specific name in the dart poison frog family (Dendrobatidae, Anura, Amphibia). RIPA 1–12.

Bejerano, G., Pheasant, M., Makunin, I., Stephen, S., Kent, W.J., Mattick, J.S., Haussler, D., 2004. Ultraconserved Elements in the Human Genome. Science 304, 1321–1325. https://doi.org/10.1126/science.1098119

Bolger, A.M., Lohse, M., Usadel, B., 2014. Trimmomatic: a flexible trimmer for Illumina sequence data. Bioinformatics 30, 2114–2120. https://doi.org/10.1093/bioinformatics/btu170

Bouckaert, R., 2010. DensiTree: making sense of sets of phylogenetic trees. Bioinformatics 26, 1372-1373. https://doi.org/10.1093/bioinformatics/btq110

Bouckaert, R., Heled, J., Kühnert, D., Vaughan, T., Wu, C.-H., Xie, D., Suchard, M.A., Rambaut, A., Drummond, A.J., 2014. BEAST 2: A Software Platform for Bayesian Evolutionary Analysis. PLOS Comput. Biol. 10, e1003537. https://doi.org/10.1371/journal.pcbi.1003537

Boulenger, G.A., 1902. Descriptions of new batrachians and reptiles from the Andes of Peru and Bolivia. Ann. Mag. Nat. Hist. 7, 394–402.

Boulenger, G.A., 1884. On a collection of frogs from Yurimaguas, Huallaga River, Northern Peru. Proc. Zool. Soc. Lond. 1883, 635–638.

Boulenger, G.A., 1882. Catalogue of the Batrachia Salientia s. Ecaudata in the Collection of the British Museum, 2nd ed. Taylor and Francis, London.

Brown, J.L., Morales, V., Summers, K., 2008. Divergence in parental care, habitat selection and larval life history between two species of Peruvian poison frogs: an experimental analysis. J. Evol. Biol. 21, 1534–1543. https://doi.org/10.1111/j.1420-9101.2008.01609.x

Brown, J.L., Siu Ting, K., von May, R., Guillory, W.X., Deutsch, M.S., Chávez, G., Twomey, E., in review. A revision of the *Ameerega rubriventris* complex (Anura: Dendrobatidae) and two new cryptic species from the East-Andean versant of Peru. Zootaxa.

Brown, J.L., Twomey, E., 2009. Complicated histories: three new species of poison frogs of the genus *Ameerega* (Anura: Dendrobatidae) from north-central Peru. Zootaxa 2049, 38.

Clough, M., Summers, K., 2000. Phylogenetic systematics and biogeography of the poison frogs: evidence from mitochondrial DNA sequences. Biol. J. Linn. Soc. 70, 515–540. https://doi.org/10.1111/j.1095-8312.2000.tb01236.x

Cochran, D.M., Goin, C.J., 1970. Frogs of Colombia. Bull. U. S. Natl. Mus. 288, 1–655.

Cope, E.D., 1874. On some Batrachia and Nematognathi brought from the upper Amazon by Prof. Orton. Proc. Acad. Nat. Sci. Phila. 26, 120–137.

Daly, J.W., McNeal, E.T., Overman, L.E., Ellison, D.H., 1985. A new class of cardiotonic agents: structure-activity correlations for natural and synthetic analogs of the alkaloid pumiliotoxin B (8-hydroxy-8-methyl-6-alkylidene-1-azabicyclo[4.3.0]nonanes). J. Med. Chem. 28, 482–486. https://doi.org/10.1021/jm00382a017

Darst, C.R., Cummings, M.E., Cannatella, D.C., 2006. A mechanism for diversity in warning signals: conspicuousness versus toxicity in poison frogs. Proc. Natl. Acad. Sci. U. S. A. 103, 5852–5857. https://doi.org/10.1073/pnas.0600625103

Drummond, A.J., Bouckaert, R., 2015. Bayesian Evolutionary Analysis with BEAST 2. Cambridge University Press, Cambridge.

Edgar, R.C., 2004. MUSCLE: multiple sequence alignment with high accuracy and high throughput. Nucleic Acids Res. 32, 1792–1797. https://doi.org/10.1093/nar/gkh340

Faircloth, B.C., 2016. PHYLUCE is a software package for the analysis of conserved genomic loci. Bioinformatics 32, 786–788. https://doi.org/10.1093/bioinformatics/btv646

Faircloth, B.C., 2013. Illumiprocessor: A Trimmomatic wrapper for parallel adapter and quality trimming.

Faircloth, B.C., McCormack, J.E., Crawford, N.G., Harvey, M.G., Brumfield, R.T., Glenn, T.C., 2012. Ultraconserved Elements Anchor Thousands of Genetic Markers Spanning Multiple Evolutionary Timescales. Syst. Biol. 61, 717–726. https://doi.org/10.1093/sysbio/sys004

French, C.M., Deutsch, M.S., Chávez, G., Almora, C.E., Brown, J.L., 2019. Speciation with introgression: Phylogeography and systematics of the *Ameerega petersi* group (Dendrobatidae). Mol. Phylogenet. Evol. 138, 31–42. https://doi.org/10.1016/j.ympev.2019.05.021

Frost, D.R., 2019. Amphibian Species of the World 6.0 [WWW Document]. URL http://research.amnh.org/vz/herpetology/amphibia/ (accessed 7.19.19).

Frost, D.R., Grant, T., Faivovich, J., Bain, R.H., Haas, A., Haddad, C.F.B., De Sá, R.O., Channing, A., Wilkinson, M., Donnellan, S.C., Raxworthy, C.J., Campbell, J.A., Blotto, B.L., Moler, P., Drewes, R.C., Nussbaum, R.A., Lynch, J.D., Green, D.M., Wheeler, W.C., 2006. The amphibian tree of life. Bull. Am. Mus. Nat. Hist. 297, 1–291. https://doi.org/10.1206/0003-0090(2006)297[0001:TATOL]2.0.CO;2

Gonzales-Álvarez, L., Lötters, S., Reichle, S., 1999. On the dendrobatid frogs from Bolivia: rediscovery of *Epipedobates bolivianus* (Boulenger, 1902), first record of *Colostethus brunneus* (Cope, 1887) and comments on other species (Anura: Dendrobatidae). Herpetozoa 12, 189–186.

Grabherr, M.G., Haas, B.J., Yassour, M., Levin, J.Z., Thompson, D.A., Amit, I., Adiconis, X., Fan, L., Raychowdhury, R., Zeng, Q., Chen, Z., Mauceli, E., Hacohen, N., Gnirke, A., Rhind, N., Palma, F. di, Birren, B.W., Nusbaum, C., Lindblad-Toh, K., Friedman, N., Regev, A., 2011. Full-length transcriptome assembly from RNA-Seq data without a reference genome. Nat. Biotechnol. 29, 644–652. https://doi.org/10.1038/nbt.1883

Grant, T., Frost, D.R., Caldwell, J.P., Gagliardo, R., Haddad, C.F.B., Kok, P.J.R., Means, D.B., Noonan, B.P., Schargel, W.E., Wheeler, W.C., 2006. Phylogenetic systematics of dart-poison frogs and their relatives (Amphibia: Athesphatanura: Dendrobatidae). Bull. Am. Mus. Nat. Hist. 299, 1–262. https://doi.org/10.1206/0003-0090(2006)299[1:PSODFA]2.0.CO;2

Grant, T., Rada, M., Anganoy-Criollo, M., Batista, A., Dias, P.H., Jeckel, A.M., Machado, D.J.,

Rueda-Almonacid, J.V., 2017. Phylogenetic systematics of dart-poison frogs and their relatives revisited (Anura: Dendrobatoidea). South Am. J. Herpetol. 12, S1–S90. https://doi.org/10.2994/SAJH-D-17-00017.1

Guillory, W.X., Muell, M.R., Summers, K., Brown, J.L., 2019. Phylogenomic reconstruction of the Neotropical poison frogs (Dendrobatidae) and their conservation. Diversity 11, 126. https://doi.org/10.3390/d11080126

Heibl, C., 2008. PHYLOCH: R language tree plotting tools and interfaces to diverse phylogenetic software packages.

Ho, S.Y.W., Duchêne, S., 2014. Molecular-clock methods for estimating evolutionary rates and timescales. Mol. Ecol. 23, 5947–5965. https://doi.org/10.1111/mec.12953

Hodges, E., Xuan, Z., Balija, V., Kramer, M., Molla, M.N., Smith, S.W., Middle, C.M., Rodesch, M.J., Albert, T.J., Hannon, G.J., McCombie, W.R., 2007. Genome-wide *in situ* exon capture for selective resequencing. Nat. Genet. 39, 1522–1527. https://doi.org/10.1038/ng.2007.42

Hoorn, C., 1994. An environmental reconstruction of the palaeo-Amazon River system (Middle–Late Miocene, NW Amazonia). Palaeogeogr. Palaeoclimatol. Palaeoecol. 112, 187–238. https://doi.org/10.1016/0031-0182(94)90074-4

Hoorn, C., 1993. Marine incursions and the influence of Andean tectonics on the Miocene depositional history of northwestern Amazonia: results of a palynostratigraphic study. Palaeogeogr. Palaeoclimatol. Palaeoecol. 105, 267–309. https://doi.org/10.1016/0031-0182(93)90087-Y

Hoorn, C., Wesselingh, F.P., ter Steege, H., Bermudez, M.A., Mora, A., Sevink, J., Sanmartin, I., Sanchez-Meseguer, A., Anderson, C.L., Figueiredo, J.P., Jaramillo, C., Riff, D., Negri, F.R., Hooghiemstra, H., Lundberg, J., Stadler, T., Sarkinen, T., Antonelli, A., 2010. Amazonia Through Time: Andean Uplift, Climate Change, Landscape Evolution, and Biodiversity. Science 330, 927–931. https://doi.org/10.1126/science.1194585

Hosner, P.A., Faircloth, B.C., Glenn, T.C., Braun, E.L., Kimball, R.T., 2016. Avoiding Missing Data Biases in Phylogenomic Inference: An Empirical Study in the Landfowl (Aves: Galliformes). Mol. Biol. Evol. 33, 1110–1125. https://doi.org/10.1093/molbev/msv347

Hsiang, A.Y., Field, D.J., Webster, T.H., Behlke, A.D., Davis, M.B., Racicot, R.A., Gauthier, J.A., 2015. The origin of snakes: revealing the ecology, behavior, and evolutionary history of early snakes using genomics, phenomics, and the fossil record. BMC Evol. Biol. 15, 87. https://doi.org/10.1186/s12862-015-0358-5

Huelsenbeck, J.P., Ronquist, F., 2001. MRBAYES: Bayesian inference of phylogenetic trees. Bioinformatics 17, 754–755. https://doi.org/10.1093/bioinformatics/17.8.754

Ješovnik, A., Sosa-Calvo, J., Lloyd, M.W., Branstetter, M.G., Fernández, F., Schultz, T.R., 2017. Phylogenomic species delimitation and host-symbiont coevolution in the fungus-farming ant genus *Sericomyrmex* Mayr (Hymenoptera: Formicidae): ultraconserved elements (UCEs) resolve a recent radiation. Syst. Entomol. 42, 523–542. https://doi.org/10.1111/syen.12228

Jungfer, K.-H., 1989. Pfeilgiftfrösche der Gattung Epipedobates mit rot granuliertem Rücken aus dem Oriente von Ecuador und Peru. Salamandra 25, 81–98.

Keping, S., Meiklejohn, K.A., Faircloth, B.C., Glenn, T.C., Braun, E.L., Kimball, R.T., 2014. The evolution of peafowl and other taxa with ocelli (eyespots): a phylogenomic approach. Proc. R. Soc. Lond. B Biol. Sci. 281. https://doi.org/10.1098/rspb.2014.0823

Knauer, F.K., 1878. Naturgeschichte der Lurche. (Amphibiologie.) Eine umfassendere Darlegung unserer Kenntnisse von dem anatomischen Bau, der Entwicklung und systematischen Eintheilung der Amphibien. A. Pichler's Witwe & Sohn, Wien.

Kumar, S., Stecher, G., Li, M., Knyaz, C., Tamura, K., Battistuzzi, F.U., 2018. MEGA X: Molecular Evolutionary Genetics Analysis across Computing Platforms. Mol. Biol. Evol. 35, 1547–1549. https://doi.org/10.1093/molbev/msy096

941 Latrubesse, E.M., Cozzuol, M., da Silva-Caminha, S.A.F., Rigsby, C.A., Absy, M.L., Jaramillo,
942 C., 2010. The Late Miocene paleogeography of the Amazon Basin and the evolution of
943 the Amazon River system. Earth-Sci. Rev. 99, 99–124.
944 https://doi.org/10.1016/j.earscirev.2010.02.005
945 Lemmon, A.R., Emme, S.A., Lemmon, E.M., 2012. Anchored hybrid enrichment for massively
946 high-throughput phylogenomics. Syst. Biol. 61, 727–744.
947 https://doi.org/10.1093/sysbio/sys049
948 Lemmon, E.M., Lemmon, A.R., 2013. High-Throughput Genomic Data in Systematics and
949 Phylogenetics. Annu. Rev. Ecol. Evol. Syst. 44, 99–121. https://doi.org/10.1146/annurev-
950 ecolsys-110512-135822
951 Limerick, S., 1980. Courtship behavior and oviposition of the poison-arrow frog *Dendrobates*
952 *pumilio*. Herpetologica 36, 69–71.
953 Liu, L., Yu, L., 2011. Estimating Species Trees from Unrooted Gene Trees. Syst. Biol. 60, 661–
954 667. https://doi.org/10.1093/sysbio/syr027
955 Lötters, S., Debold, P., Henle, K., Glaw, F., Kneller, M., 1997. Ein neuer Pfeilgiftfrosch aus der
956 *Epipedobates pictus*-Gruppe vom Osthang der Cordillera Azul in Perú. Herpetofauna 19,
957 25–34.
958 Lötters, S., Jungfer, K.-H., Henkel, F.W., Schmidt, W., 2007. Poison Frogs: Biology, Species &
959 Captive Husbandry. Chimaira, Frankfurt.
960 Lötters, S., Schmitz, A., Reichle, S., Rödder, D., Quennet, V., 2009. Another case of cryptic
961 diversity in poison frogs (Dendrobatidae: *Ameerega*)—description of a new species from
962 Bolivia. Zootaxa 20–30.
963 Lozano, C.M., 2015. Niceforo's Poison Frog, *Ameerega ingeri* (Cochran & Goin, 1970), in:
964 Kahn, T.R., La Marca, E., Lötters, S., Brown, J.L., Twomey, E., Amézquita, A. (Eds.),
965 Aposematic Poison Frogs (Dendrobatidae) of the Andean Countries: Bolivia, Colombia,
966 Ecuador, Peru and Venezuela, Conservation International Tropical Field Guide Series.
967 Conservation International, Arlington, pp. 161–165.
968 Lutz, A., 1925. Batraciens du Brésil. Comptes Rendus Mém. Hebd. Séances Société Biol. Ses
969 Fil. 2, 137–139.
970 Maan, M.E., Cummings, M.E., 2009. Sexual dimorphism and directional sexual selection on
971 aposematic signals in a poison frog. Proc. Natl. Acad. Sci. 106, 19072–19077.
972 https://doi.org/10.1073/pnas.0903327106
973 Mebs, D., Jansen, M., Köhler, G., Pogoda, W., Kauert, G., 2010. Myrmecophagy and alkaloid
974 sequestration in amphibians: a study on *Ameerega picta* (Dendrobatidae) and
975 *Elachistocleis sp.* (Microhylidae) frogs. Salamandra 46, 11–15.
976 Meiklejohn, K.A., Faircloth, B.C., Glenn, T.C., Kimball, R.T., Braun, E.L., 2016. Analysis of a
977 Rapid Evolutionary Radiation Using Ultraconserved Elements: Evidence for a Bias in
978 Some Multispecies Coalescent Methods. Syst. Biol. 65, 612–627.
979 https://doi.org/10.1093/sysbio/syw014
980 Melin, D.E., 1941. Contributions to the knowledge of the Amphibia of South America. Göteb. K.
981 Vetensk.-Och Vitterh.-Samh. Handl. Serien B Mat. Och Naturvetenskapliga Skr. 1, 1–71.
982 Mello, B., Tao, Q., Tamura, K., Kumar, S., 2017. Fast and Accurate Estimates of Divergence
983 Times from Big Data. Mol. Biol. Evol. 34, 45–50. https://doi.org/10.1093/molbev/msw247
984 Miller, M.R., Dunham, J.P., Amores, A., Cresko, W.A., Johnson, E.A., 2007. Rapid and cost-
985 effective polymorphism identification and genotyping using restriction site associated
986 DNA (RAD) markers. Genome Res. 17, 240–248. https://doi.org/10.1101/gr.5681207
987 Minh, B.Q., Nguyen, M.A.T., von Haeseler, A., 2013. Ultrafast Approximation for Phylogenetic
988 Bootstrap. Mol. Biol. Evol. 30, 1188–1195. https://doi.org/10.1093/molbev/mst024
989 Mirarab, S., Reaz, R., Bayzid, Md.S., Zimmermann, T., Swenson, M.S., Warnow, T., 2014.
990 ASTRAL: genome-scale coalescent-based species tree estimation. Bioinformatics 30,
991 i541–i548. https://doi.org/10.1093/bioinformatics/btu462

Morales, V.R., Velazco, P.M., 1998. Una especie nueva de *Epipedobates* (Amphibia, Anura, Dendrobatidae) de Perú. Amphib-Reptil. 19, 369–376.
Myers, C.W., 1987. New generic names from some neotropical poison frogs (Dendrobatidae). Papéis Avulsos Zool. Mus. Zool. Universidade São Paulo 36, 301–306.
Myers, C.W., 1982. Spotted Poison Frogs: Descriptions of Three New *Dendrobates* from Western Amazonia, and Resurrection of a Lost Species from “Chiriqui.” Am. Mus. Novit. 23.
Myers, C.W., Daly, J.W., Malkin, B., 1978. A dangerously toxic new frog (*Phyllobates*) used by Emberá Indians of western Colombia, with discussion of blowgun fabrication and dart poisoning. Bull. Am. Mus. Nat. Hist. 161, 307–366.
Myers, C.W., Rodríguez, L.O., Icochea, J., 1998. *Epipedobates simulans*, a new cryptic species of Poison Frog from southeastern Peru, with notes on *E. macero* and *E. petersi* (Dendrobatidae). Am. Mus. Novit. 1–20.
Neves, M.O., Da Silva, L.A., Akieda, P.S., Cabrera, R., Koroiva, R., Santana, D.J., 2017. A new species of poison frog, genus *Ameerega* (Anura: Dendrobatidae), from the southern Amazonian rain forest. Salamandra 53, 485–493.
Nguyen, L.-T., Schmidt, H.A., von Haeseler, A., Minh, B.Q., 2015. IQ-TREE: A Fast and Effective Stochastic Algorithm for Estimating Maximum-Likelihood Phylogenies. Mol. Biol. Evol. 32, 268–274. https://doi.org/10.1093/molbev/msu300
Noonan, B.P., Gaucher, P., 2006. Refugial isolation and secondary contact in the dyeing poison frog *Dendrobates tinctorius*. Mol. Ecol. 15, 4425–4435. https://doi.org/10.1111/j.1365-294X.2006.03074.x
Okou, D.T., Steinberg, K.M., Middle, C., Cutler, D.J., Albert, T.J., Zwick, M.E., 2007. Microarray-based genomic selection for high-throughput resequencing. Nat. Methods 4, 907–909. https://doi.org/10.1038/nmeth1109
Paradis, E., Claude, J., Strimmer K., 2004. APE: Analyses of Phylogenetics and Evolution in R language. Bioinformatics, 20, 289-290. https://doi.org/10.1093/bioinformatics/btg412
Padial, J.M., Chaparro, J.C., Castroviejo-Fisher, S., Guayasamin, J.M., Lehr, E., Delgado, A.J., Vaira, M., Teixeira, M., Aguayo, R., De la Riva, I., 2012. A revision of species diversity in the neotropical genus *Oreobates* (Anura: Strabomantidae), with the description of three new species from the Amazonian slopes of the Andes. Am. Mus. Novit. 3752, 1–55.
Persons, N.W., Hosner, P.A., Meiklejohn, K.A., Braun, E.L., Kimball, R.T., 2016. Sorting out relationships among the grouse and ptarmigan using intron, mitochondrial, and ultra-conserved element sequences. Mol. Phylogenet. Evol. 98, 123–132. https://doi.org/10.1016/j.ympev.2016.02.003
Pfennig, D.W., Mullen, S.P., 2010. Mimics without models: causes and consequences of allopatry in Batesian mimicry complexes. Proc. R. Soc. B Biol. Sci. 277, 2577–2585. https://doi.org/10.1098/rspb.2010.0586
Prates, I., Antoniazzi, M.M., Sciani, J.M., Pimenta, D.C., Toledo, L.F., Haddad, C.F.B., Jared, C., 2012. Skin glands, poison and mimicry in dendrobatid and leptodactylid amphibians. J. Morphol. 273, 279–290. https://doi.org/10.1002/jmor.11021
Pyron, A.R., Wiens, J.J., 2011. A large-scale phylogeny of Amphibia including over 2800 species, and a revised classification of extant frogs, salamanders, and caecilians. Mol. Phylogenet. Evol. 61, 543–583. https://doi.org/10.1016/j.ympev.2011.06.012
Rambaut, A., Drummond, A.J., Xie, D., Baele, G., Suchard, M.A., 2018. Posterior Summarization in Bayesian Phylogenetics Using Tracer 1.7. Syst. Biol. 67, 901–904. https://doi.org/10.1093/sysbio/syy032
Roberts, J.L., Brown, J.L., May, R. von, Arizabal, W., Schulte, R., Summers, K., 2006. Genetic divergence and speciation in lowland and montane Peruvian poison frogs. Mol. Phylogenet. Evol. 41, 149–164. https://doi.org/10.1016/j.ympev.2006.05.005
Rodríguez, L.O., Myers, C.W., 1993. A New Poison Frog from Manu National Park,

1043 Southeastern Peru (Dendrobatidae, *Epipedobates*). Am. Mus. Novit. 1–15.
1044 Rull, V., 2011. Neotropical biodiversity: timing and potential drivers. Trends Ecol. Evol. 26, 508–
1045 513. https://doi.org/10.1016/j.tree.2011.05.011
1046 Santos, J.C., Coloma, L.A., Cannatella, D.C., 2003. Multiple, recurring origins of aposematism
1047 and diet specialization in poison frogs. Proc. Natl. Acad. Sci. 100, 12792–12797.
1048 https://doi.org/10.1073/pnas.2133521100
1049 Santos, J.C., Coloma, L.A., Summers, K., Caldwell, J.P., Ree, R., Cannatella, D.C., 2009.
1050 Amazonian amphibian diversity Is primarily derived from late Miocene Andean lineages.
1051 PLoS Biol. 7, e1000056. https://doi.org/10.1371/journal.pbio.1000056
1052 Santos, J.C., Tarvin, R.D., O'Connell, L.A., 2016. A Review of Chemical Defense in Poison
1053 Frogs (Dendrobatidae): Ecology, Pharmacokinetics, and Autoresistance, in: Schulte,
1054 B.A., Goodwin, T.E., Ferkin, M.H. (Eds.), Chemical Signals in Vertebrates 13. Springer
1055 International Publishing, pp. 305–337.
1056 Schlegel, H., 1826. Notice sur l'Erpétologie de l'île de Java; par M. Boïé (Ouvrage manuscript).
1057 Bull. Sci. Nat. Géologie Serie 2, 233–240.
1058 Schulte, R., 1999. Pfeilgiftfrösche: "Artenteil - Peru." Karl Hauck, Waiblingen.
1059 Schulte, R., 1989. Nueva especie de rana venenosa del genero *Epipedobates* registrada en la
1060 Cordillera Oriental, Departamento de San Martin. Bol. Lima 63, 41–46.
1061 Serrano-Rojas, S.J., Whitworth, A., Villacampa, J., May, R.V., Padial, J.M., Chaparro, J.C.,
1062 2017. A new species of poison-dart frog (Anura: Dendrobatidae) from Manu province,
1063 Amazon region of southeastern Peru, with notes on its natural history, bioacoustics,
1064 phylogenetics, and recommended conservation status. Zootaxa 4221, 71.
1065 https://doi.org/10.11646/zootaxa.4221.1.3
1066 Silverstone, P.A., 1976. A Revision of the Poison-Arrow Frogs of the Genus *Phyllobates* Bibron
1067 in Sagra (Family Dendrobatidae). Nat. Hist. Mus. Los Angel. Cty. Sci. Bull. 27, 1–53.
1068 Silverstone, P.A., 1975. A revision of the poison-arrow frogs of the genus *Dendrobates* Wagler.
1069 Nat. Hist. Mus. Los Angel. Cty. Sci. Bull. 21, 1–55.
1070 Solís-Lemus, C., Ané, C., 2016. Inferring Phylogenetic Networks with Maximum
1071 Pseudolikelihood under Incomplete Lineage Sorting. PLOS Genet. 12, e1005896.
1072 https://doi.org/10.1371/journal.pgen.1005896
1073 Spix, J.B. von, 1824. Animalia Nova sive species novae Testudinum Ranarum, quas in itinere
1074 per Brasiliam annis MDCCCXVII - MDCCCXX jussu et auspiciis Maximiliani Josephi I.
1075 Bavariae regis. - Monachii: 4pp, 1-53, pis. 1-17 + 1-22. F. S. Hübschmann, München.
1076 Steindachner, F., 1864. Batrachologische Mittheilungen. Verhandlungen Zool.-Bot. Ver. Wien
1077 239–288.
1078 Streicher, J.W., Wiens, J.J., 2017. Phylogenomic analyses of more than 4000 nuclear loci
1079 resolve the origin of snakes among lizard families. Biol. Lett. 13, 20170393.
1080 https://doi.org/10.1098/rsbl.2017.0393
1081 Streicher, J.W., Wiens, J.J., 2016. Phylogenomic analyses reveal novel relationships among
1082 snake families. Mol. Phylogenet. Evol. 100, 160–169.
1083 https://doi.org/10.1016/j.ympev.2016.04.015
1084 Summers, K., Clough, M.E., 2001. The evolution of coloration and toxicity in the poison frog
1085 family (Dendrobatidae). Proc. Natl. Acad. Sci. 98, 6227–6232.
1086 https://doi.org/10.1073/pnas.101134898
1087 Summers, K., Symula, R., Clough, M., Cronin, T., 1999. Visual mate choice in poison frogs.
1088 Proc. R. Soc. B Biol. Sci. 266, 2141–2145. https://doi.org/10.1098/rspb.1999.0900
1089 Symula, R., Schulte, R., Summers, K., 2002. Molecular phylogenetic evidence for a mimetic
1090 radiation in Peruvian poison frogs supports a Müllerian mimicry hypothesis. Proc. Biol.
1091 Sci. 268, 2415–21. https://doi.org/10.1098/rspb.2001.1812
1092 Tagliacollo, V.A., Lanfear, R., 2018. Estimating Improved Partitioning Schemes for

1093 Ultraconserved Elements. Mol. Biol. Evol. 35, 1798–1811.
1094 https://doi.org/10.1093/molbev/msy069
1095 Tamura, K., Battistuzzi, F.U., Billing-Ross, P., Murillo, O., Filipski, A., Kumar, S., 2012.
1096 Estimating divergence times in large molecular phylogenies. Proc. Natl. Acad. Sci. 109,
1097 19333–19338. https://doi.org/10.1073/pnas.1213199109
1098 Tarvin, R.D., Borghese, C.M., Sachs, W., Santos, J.C., Lu, Y., O'Connell, L.A., Cannatella,
1099 D.C., Harris, R.A., Zakon, H.H., 2017. Interacting amino acid replacements allow poison
1100 frogs to evolve epibatidine resistance. Science 357, 1261–1266.
1101 https://doi.org/10.1126/science.aan5061
1102 Tarvin, R.D., Santos, J.C., O'Connell, L.A., Zakon, H.H., Cannatella, D.C., 2016. Convergent
1103 Substitutions in a Sodium Channel Suggest Multiple Origins of Toxin Resistance in
1104 Poison Frogs. Mol. Biol. Evol. 33, 1068–1081. https://doi.org/10.1093/molbev/msv350
1105 Twomey, E., Brown, J.L., 2008. A partial revision of the *Ameerega hahneli* complex (Anura:
1106 Dendrobatidae) and a new cryptic species from the East-Andean versant of Central
1107 Peru. Zootaxa 1757, 49–65.
1108 Twomey, E., Vestergaard, J.S., Summers, K., 2014. Reproductive isolation related to mimetic
1109 divergence in the poison frog *Ranitomeya imitator*. Nat. Commun. 5, 4749.
1110 https://doi.org/10.1038/ncomms5749
1111 Twomey, E., Vestergaard, J.S., Venegas, P.J., Summers, K., 2016. Mimetic Divergence and the
1112 Speciation Continuum in the Mimic Poison Frog *Ranitomeya imitator*. Am. Nat. 187,
1113 205–224. https://doi.org/10.1086/684439
1114 Vaz-Silva, W., Maciel, N.M., 2011. A new cryptic species of *Ameerega* (Anura: Dendrobatidae)
1115 from Brazilian Cerrado. Zootaxa 57–68.
1116 Vences, M., Kosuch, J., Boistel, R., Haddad, C.F.B., La Marca, E., Lötters, S., Veith, M., 2003.
1117 Convergent evolution of aposematic coloration in Neotropical poison frogs: a molecular
1118 phylogenetic perspective. Org. Divers. Evol. 3, 215–226. https://doi.org/10.1078/1439-
1119 6092-00076
1120 Vences, M., Kosuch, J., Lötters, S., Widmer, A., Jungfer, K.-H., Köhler, J., Veith, M., 2000.
1121 Phylogeny and classification of poison frogs (Amphibia: Dendrobatidae), Based on
1122 mitochondrial 16S and 12S ribosomal RNA gene sequences. Mol. Phylogenet. Evol. 15,
1123 34–40. https://doi.org/10.1006/mpev.1999.0738
1124 Wagler, J.G., 1830. Natürliches System der Amphibien : mit vorangehender Classification der
1125 Säugethiere und Vögel: ein Beitrag zur vergleichenden Zoologie. J. G. Cotta, München,
1126 Stuttgart, and Tübingen.
1127 Wang, I.J., Shaffer, H.B., 2008. Rapid color evolution in an aposematic species: A phylogenetic
1128 analysis of color variation in the strikingly polymorphic strawberry poison-dart frog.
1129 Evolution 62, 2742–2759. https://doi.org/10.1111/j.1558-5646.2008.00507.x
1130 Wang, Z., Gerstein, M., Snyder, M., 2009. RNA-Seq: a revolutionary tool for transcriptomics.
1131 Nat. Rev. Genet. 10, 57–63. https://doi.org/10.1038/nrg2484
1132 Wells, K.D., 1980. Behavioral ecology and social organization of a dendrobatid frog
1133 (*Colostethus inguinalis*). Behav. Ecol. Sociobiol. 6, 199–209.
1134 Winker, K., Glenn, T.C., Faircloth, B.C., 2018. Ultraconserved elements (UCEs) illuminate the
1135 population genomics of a recent, high-latitude avian speciation event. PeerJ 6, e5735.
1136 https://doi.org/10.7717/peerj.5735
1137 Zhang, C., Rabiee, M., Sayyari, E., Mirarab, S., 2018. ASTRAL-III: polynomial time species tree
1138 reconstruction from partially resolved gene trees. BMC Bioinformatics 19, 153.
1139 https://doi.org/10.1186/s12859-018-2129-y
1140 Zhu, J., Nakhleh, L., 2018. Inference of species phylogenies from bi-allelic markers using
1141 pseudo-likelihood. Bioinformatics 34, i376–i385.
1142 https://doi.org/10.1093/bioinformatics/bty295
1143 Zimmermann, H., Zimmermann, E., 1988. Etho-Taxonomie und zoogeographische

Artengruppenbildung bei Pfeilgiftfroschen (Anura: Dendrobatidae). Salamandra 24, 125–160.

Captions for supplementary material

Table S1: List of samples used to extract genomic DNA for phylogenetic analysis and associated localities for each sample. The samples are arranged in the same order as in the ML tree in Fig. S1. Sequence IDs correspond to the tip labels of the tree for ease of reference. The "No. loci" column shows the number of UCE loci captured for that sample, before any filtering of alignments for completeness or informativeness.

Table S2: Exact mean divergence dates and associated uncertainty values for each node of the phylogenies shown in Figures 3 and S7. Values for both BEAST 2 analyses (200 most informative loci vs. 200 random loci) and the RelTime analysis (based on the 200 most informative loci) are shown. Uncertainty values for BEAST 2 represent 95% highest posterior density intervals, while for RelTime they represent 95% confidence intervals. The leftmost column "Node" provides the number used to identify each node, and matches the node numbers shown in Fig. 3. In RelTime, 95% confidence interval estimates for the selected outgroup taxon (in this case, *Silverstoneia nubicola*) are not provided. Note that the topology of the 200 random loci BEAST 2 tree is nonidentical to the other trees, so that direct comparisons between certain node numbers are not applicable.

Figure S1: Maximum-likelihood tree generated in IQ-TREE using the comprehensive dataset (n = 104). Only bootstrap values below 100% are shown. Each sample is assigned to a putative species, shown as a black clade label to the right of the tree. Most species are assigned to a species group (colored clade labels) as shown in Fig. 1. Note that although *Ameerega picta, A. trivittata,* and *A. pulchripecta* form a clade in this tree, they are not assigned to their own species group because this result was not found consistently using other methods and datasets (see Figs. S2 and S3).

Figure S2: Comparison of trees generated from IQ-TREE and ASTRAL-III. Both trees were generated from the restricted dataset (n = 35, one sample per species). The ASTRAL-III tree summarizes gene trees constructed from the 200 most parsimonious UCE loci from this dataset. The IQ-TREE tree was constructed from 1,067 UCE loci, retained after filtering for loci with 8 < PIS < 50. ASTRAL-III support values are in local posterior probabilities, while IQ-TREE support is shown in bootstrap values; thus support is not directly comparable between the two trees.. Differences in topology are highlighted in gray. The ASTRAL tree is the same one shown on the left side of Figs. S3 and S4.

Figure S3: Comparison of the two trees generated in ASTRAL-III. The right tree was made with the comprehensive dataset consisting of all 104 samples, each assigned to one of 35 putative species in a mapping file provided to ASTRAL. Each species is collapsed to a single tip. Differences in topology are highlighted in gray. Node labels show branch support in local posterior probabilities. The left tree is the same one shown on the left side of Fig. S2.

Figure S4: Comparison of two trees generated in ASTRAL-III from the restricted dataset (one sample per species). The left tree was made with the 200 most parsimony-informative loci for that dataset. The right tree was made with all 1,067 loci remaining after filtering for 8 < PIS < 50. Differences in topology are highlighted in gray. Node labels show branch support in local posterior probabilities. The left tree is the same one shown on the left side of Fig. S2.

Figure S5: Visualization of high levels of gene tree discordance in *Ameerega.* a. The three "most likely" tree topologies as inferred by Densitree. Blue is most likely, red is second-most, and green third-most. This panel illustrates gene tree topological discordance in only a few trees. Taxon labels include the sequence ID in parentheses connecting the sample to its relevant information in Table S1. b. "Tree cloud" of gene trees constructed in IQ-TREE, time-calibrated in APE, and visualized in Densitree. This simply illustrates the large gene tree topological discordance in our dataset. No clear pattern arises from a visualization of all trees. c. ASTRAL-III topology constructed from the gene trees shown in part b. The topology is remarkably similar to that retrieved in more comprehensive analyses (see Figs. S1, S2, etc.), despite much-reduced taxon and locus sampling. Only node labels, representing local posterior probabilities, below 100% are shown. This illustrates that even given massive gene tree discordance, coalescent summary methods can still converge on consensus species tree topologies.

Figure S6: Four-panel map showing the distribution of samples used in the study. The map is identical to Figure 2, but each panel shows a rough evolutionary group, allowing for better context and ease of reading. A. The *macero, petersi,* and *simulans* groups, located mostly in southeastern Peru. B. The *hahneli* group, located throughout Amazonia. C. The *parvula* and *bassleri* groups, and *Ameerega ingeri,* located from east-central Peru up into southwestern Colombia. D. The *braccata* group as well as "miscellaneous" species that are not assigned to any species group, located throughout Amazonia down through Bolivia and the Brazilian savannah.

Figure S7: Comparison of all three divergence time estimations performed in the study (identical to Fig. 3, but with the addition of the BEAST 2 tree from 200 random loci). The top tree was calibrated in BEAST 2 from the 200 most informative loci, and constrained to the topology of the restricted dataset ASTRAL-III tree from the 200 most informative loci (Fig. S2). The middle tree was also calibrated in BEAST 2, but from 200 random loci, and instead constrained to the topology of the restricted dataset ASTRAL-III tree from all loci (after filtering for loci with 8 < PIS < 50; n = 1,067) (Fig. S4). The bottom tree was calibrated in RelTime (implemented in MEGA X) from the 200 most informative loci, constrained to the topology of the restricted dataset ASTRAL-III tree from the 200 most informative loci (same as the top tree). Error bars, shown in gray, represent 95% highest posterior density intervals (in the case of BEAST 2) or 95% confidence intervals (RelTime). All scale bars are in units of millions of years ago (Ma). Each node is assigned a number which is referenced in Table S2, where exact values for node heights and error bar estimates are provided. The calibration node was Node 2 in all analyses.

Note that the 200 random loci BEAST 2 tree's topology is not identical to the others (which are identical), so comparisons between specific nodes may not be applicable.